Infrared microspectroscopy for environmental science: from the basis to data analysis and results' interpretation

Lisa Vaccari
SISSI beamline @ Elettra Laboratory

Advanced School on Synchrotron Techniques in Environmental Scientific Projects

SESAME

elettra

Talk outline

- Introduction
  - The infrared spectral region
  - Basics on vibrational spectroscopy
- Instrumentation
  - FTIR interferometer
  - Vis-IR microscope
  - InfraRed Synchrotron Radiation (IRSR)
    - Infrared Synchrotron Radiation sources
    - IRSR Advantages
    - IR Beamline design
- FTIR spectroscopy for environmental sciences
- Biological information from a FTIR microspetrum
- From the sample to the biological information
  - Sampling techniques
  - Sample preparation
  - Data acquisition
  - Data analysis
- Some examples
  - Real-time Chemical imaging of bacterial activity in biofilms
  - In Situ FT-IR Microscopic Study on Enzymatic Treatment of poplar Wood Cross-Sections
  - Transmissible spongiform encephalopathies

The infrared spectral region

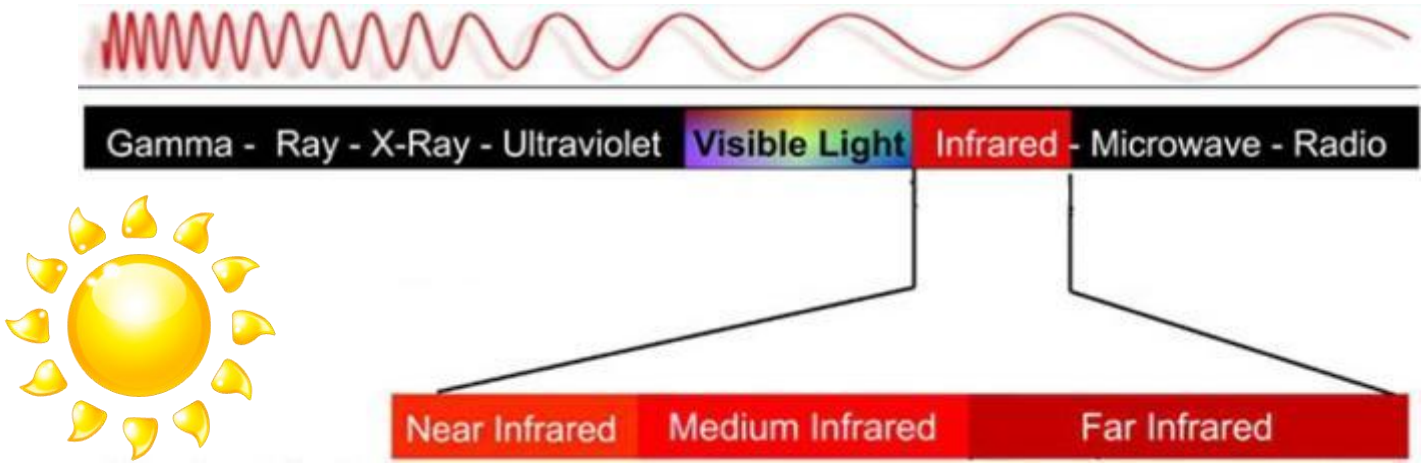

	NIR	MIR		FIR
λ (μm)	0.74	3	30	300
ν (THz)	400	100	10	1
$\bar{\nu}$ (cm^{-1})	~13000	~3333	~333	~33
E (eV)	1.65	0.413	0.041	0.004
E (Kcal/mol)	37	10	1	0.1

The IR spectral range is a wide region of long wavelengths

Basics on vibrational spectroscopy

IR spectroscopy is an absorption spectroscopy

Direct resonance between vibrational transition frequency and photon frequency

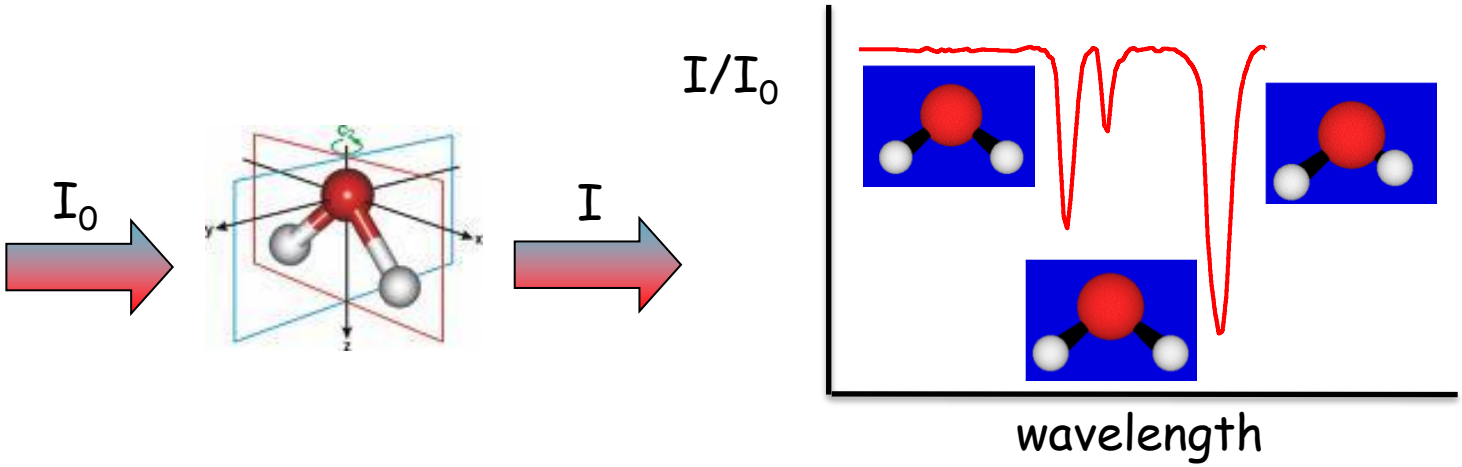

Vibrational (stretching) frequencies

For a diatomic molecule or molecular fragment

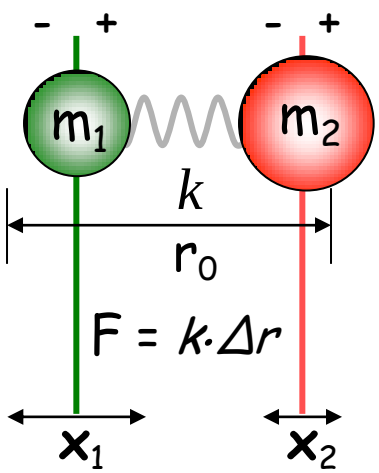

$$\nu = \frac{1}{2\pi}\sqrt{\frac{k}{\mu}}$$

$$\mu = \text{Reduced mass} = \frac{m_1 m_2}{m_1 + m_2}$$

$$K = \text{Spring constant}$$

$$\Delta r = \text{Displacement}$$

Vibrational energies

Harmonic approximation

$$E_{vib} = h\nu_0(n+1/2),\ \nu_0 = \text{fudamental vibrational frequancy} = \frac{1}{2\pi}\sqrt{\frac{k}{\mu}}$$

Anharmonicity

$$E_{vib} = h\nu_0[(n+1/2) - x_o(n+1/2)^2 + \text{higher terms}]$$

$$x_0 = \text{anharmonic constant}$$

Harmonic oscillator

$$\Delta n = 1$$

Anharmonic oscillator

$$\Delta n = \text{integer}$$

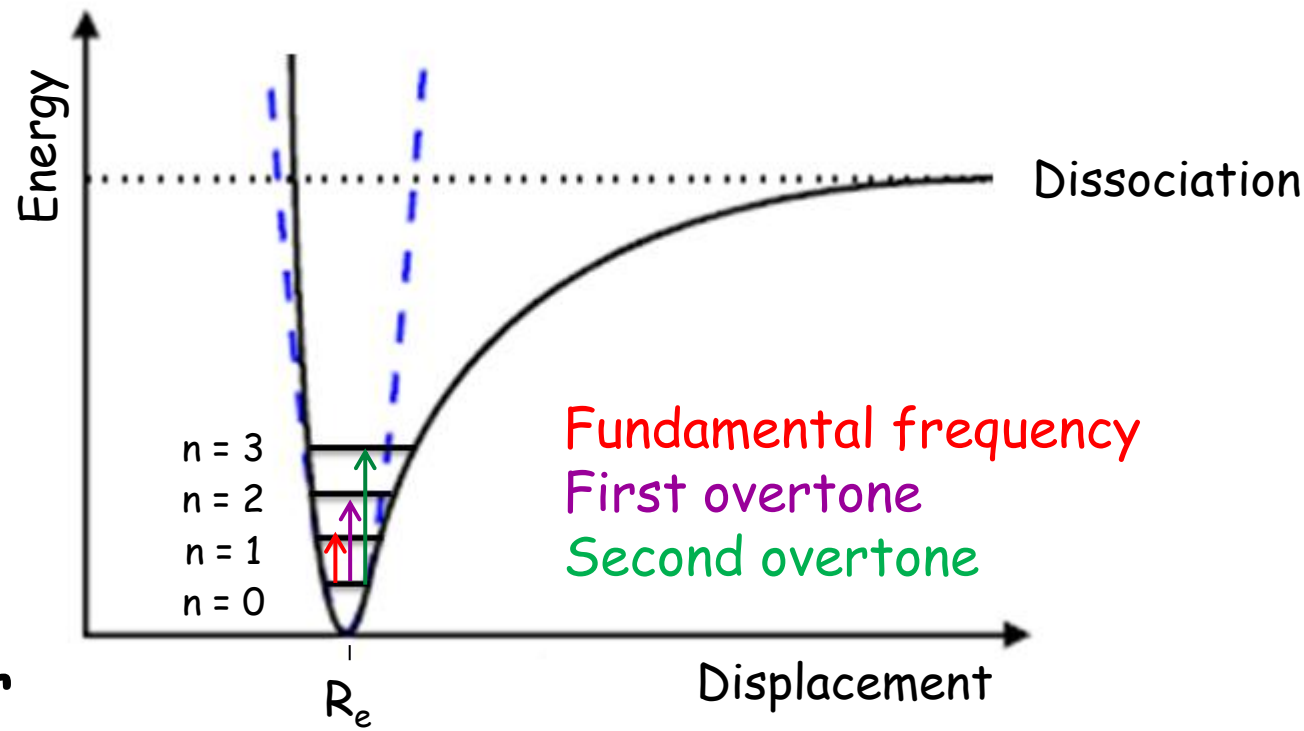

Fundamental modes of vibrations for polyatomic molecules

Linear N-atom molecule: 3N-5 modes of vibration

Non linear N-atom molecule: 3N-6 modes of vibration

Symmetric Stretching

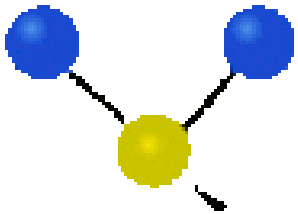

Antisymmetric Stretching

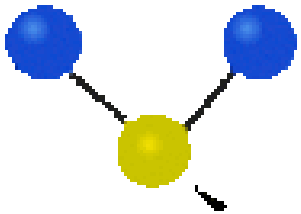

Scissoring

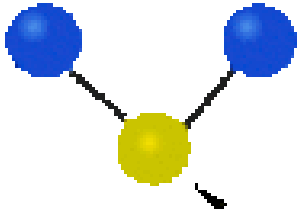

Rocking

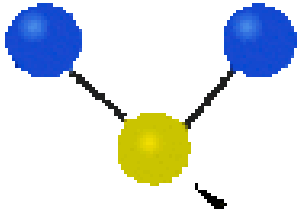

Wagging

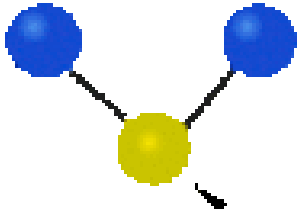

Twisting

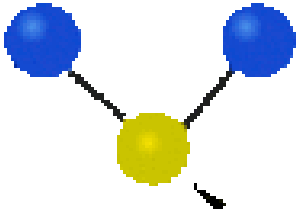

Only the vibrational modes that produce a change of the molecular dipole moment are IR active

The liquid water absorption spectrum

Overtones and combination bands

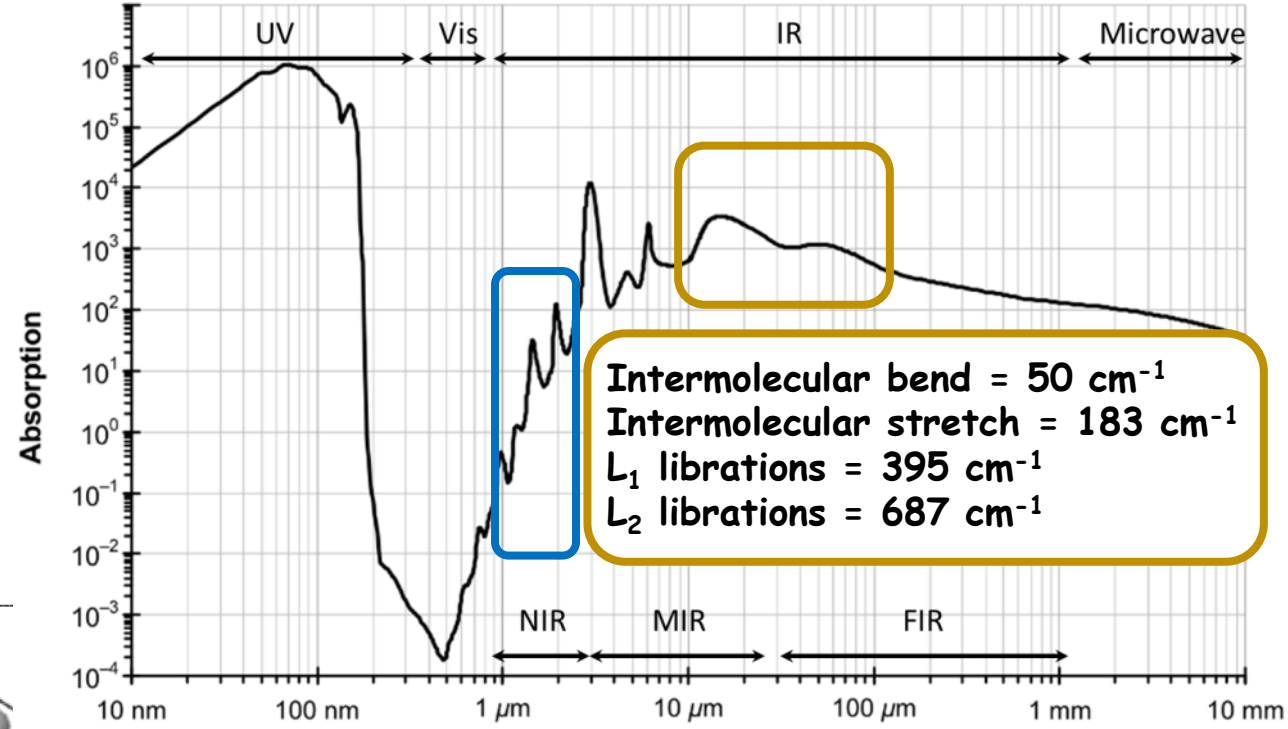

Intermolecular bend = 50 cm^{-1}
Intermolecular stretch = 183 cm^{-1}
L_1 librations = 395 cm^{-1}
L_2 librations = 687 cm^{-1}

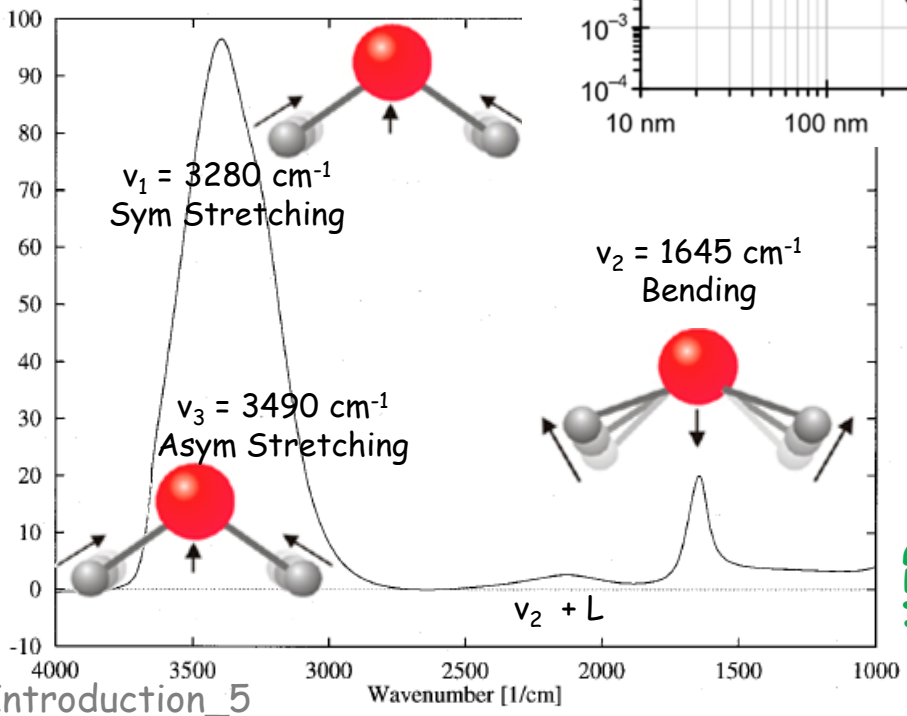

MIR water spectrum

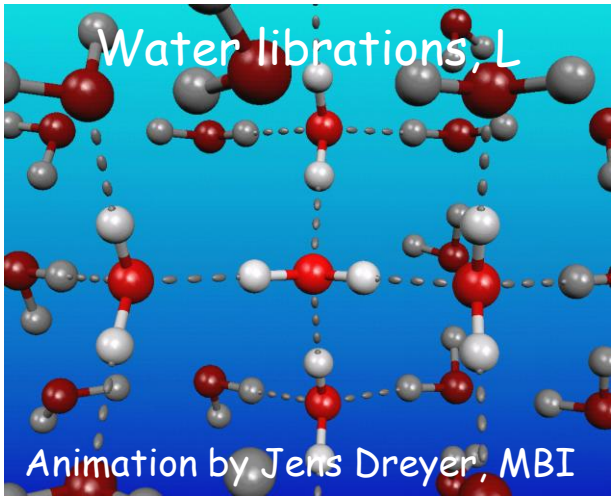

FTIR interferometer

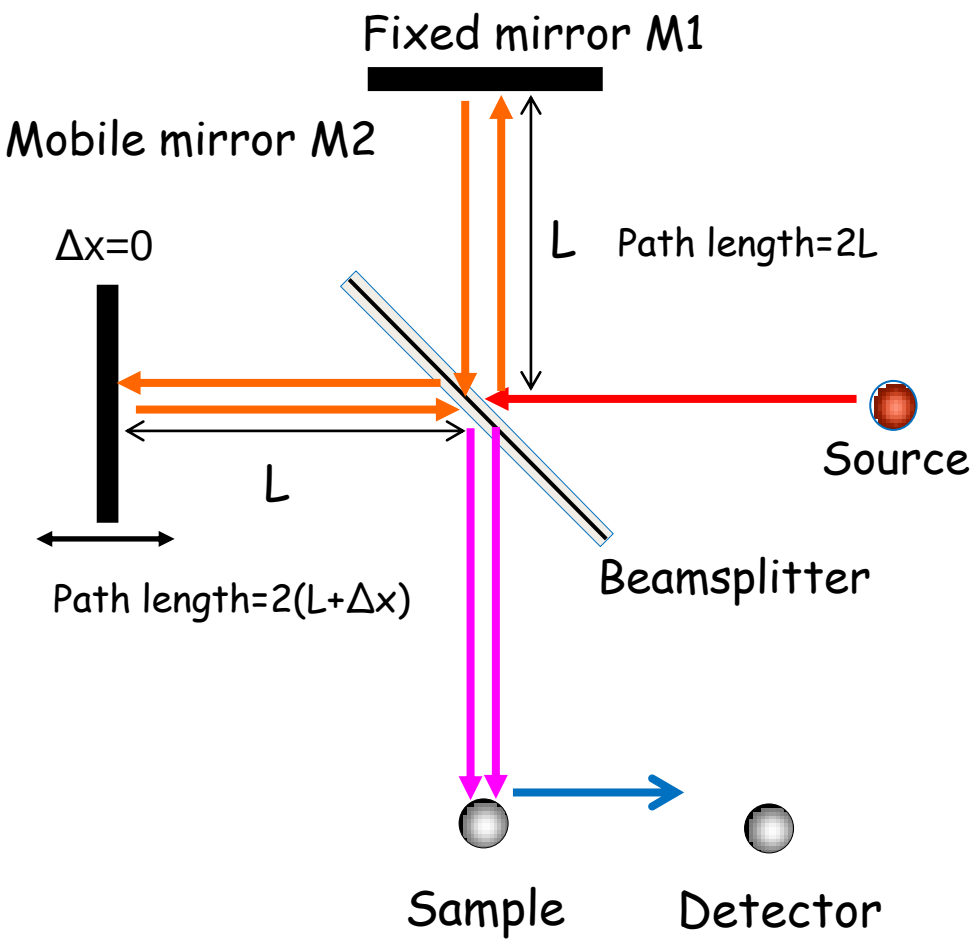

Spectral Resolution

$\Delta\nu \sim 1/\Delta x$ (cm^{-1}) ~ 0.001 cm^{-1} ~ 1meV

Conventional sources

NIR: Tungsten lamp
MIR: Glow bar (SiC)
FIR: Hg-Arc

Beamsplitters

NIR: CaF_2
MIR: KBr
FIR: Mylar, Silicon

Detectors

NIR – InGaAs, InSb, Ge, Si room temperature detectors
MIR: Room temperature DLaTGS
Nitrogen cooled MCT
FIR – He Cooled Silicon Bolometer
Room temperature DLaTGS

Origin of the interferogram

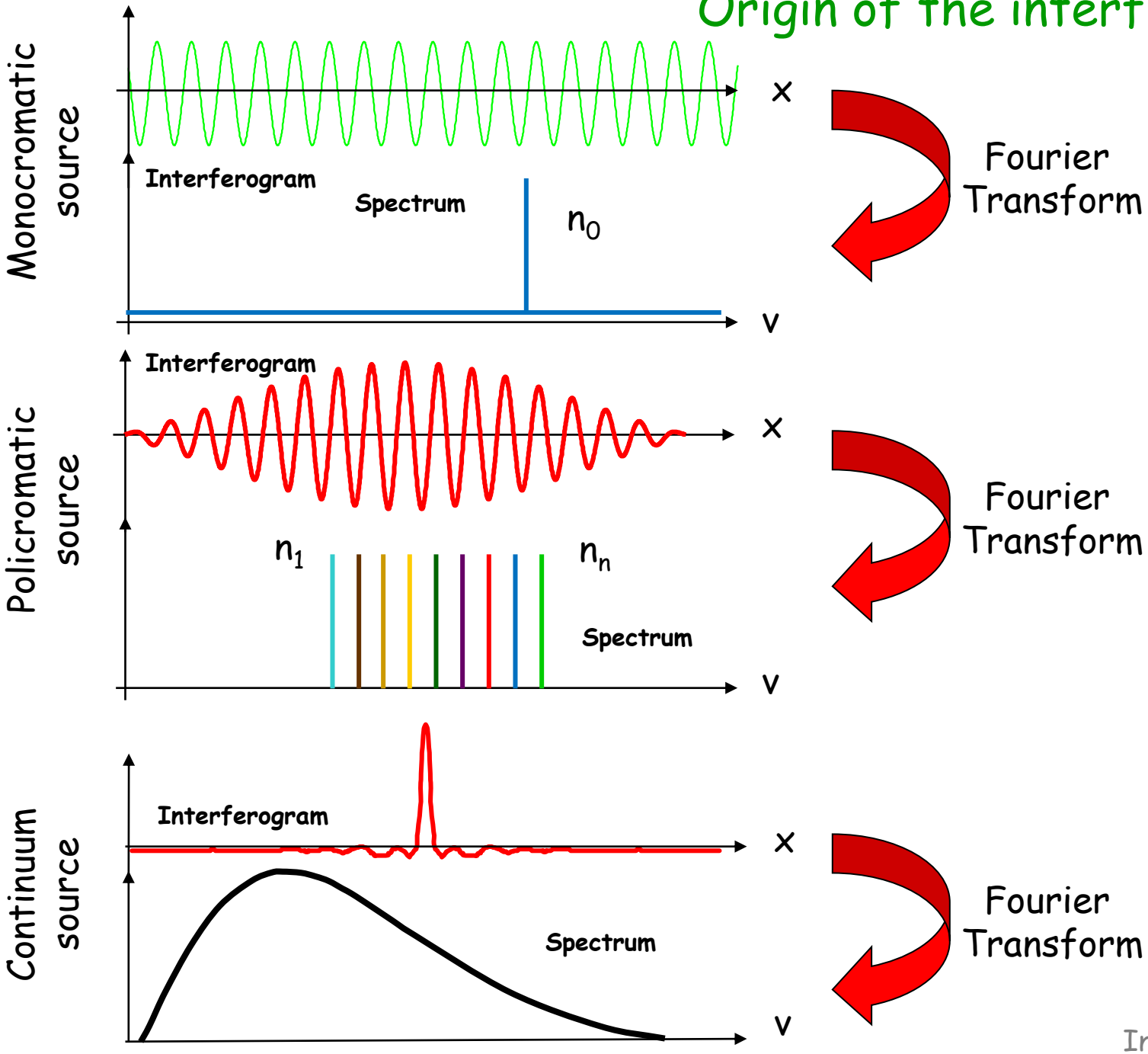

Advantages of FTIR interferometers

- Jacquinot's throughput advantage
  - All source wavelengths are measured simultaneously in an interferometer, whereas in a dispersive spectrometer they are measured successively. A complete spectrum can be collected very rapidly and many scans can be averaged in the time taken for a single scan of a dispersive spectrometer.
- Fellgett's Advantage (Multiplex advantage)
  - For the same resolution, the energy throughput in an interferometer can be higher than in a dispersive spectrometer, where it is restricted by the slits.
- Connes' accuracy advantage
  - The wavenumber scale of an interferometer is derived from a HeNe laser that acts as an internal reference for each scan. The wavenumber of this laser is known very accurately and is very stable. As a result, the wavenumber calibration of interferometers is much more accurate and has much better long term stability than the calibration of dispersive instruments.

As a result, a FTIR spectrum can be measured with the same signal-to-noise ratio than a dispersive spectrum in a much shorter time (seconds rather than minutes) and spectral subtractions can be carried out without frequency errors

Vis-IR microscopes

Spatially resolved chemical information on heterogeneous samples are obtained by coupling FTIR spectrometers with specially designed Vis-IR microscopes

Schwarzschild objective

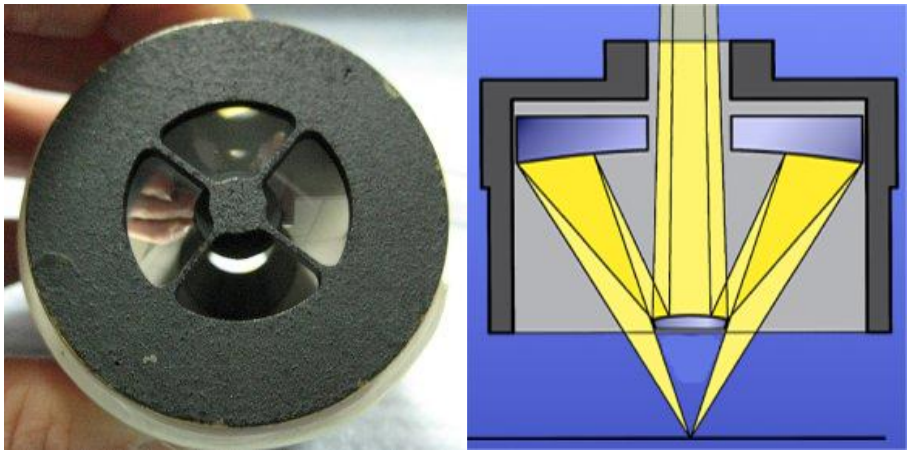

The highest achievable lateral resolution, δ, is diffraction limited

Objective NA	Wavelength	δ
0.4	10 μm (1000cm^{-1})	~15 μm
	2.5 μm (4000cm^{-1})	~ 4 μm
0.65	10 μm (1000cm^{-1})	~ 9,5 μm
	2.5 μm (4000cm^{-1})	~ 2,5 μm

$$\delta \approx 0.61\,\lambda / NA$$

FTIR mapping versus FTIR imaging

Mapping layout

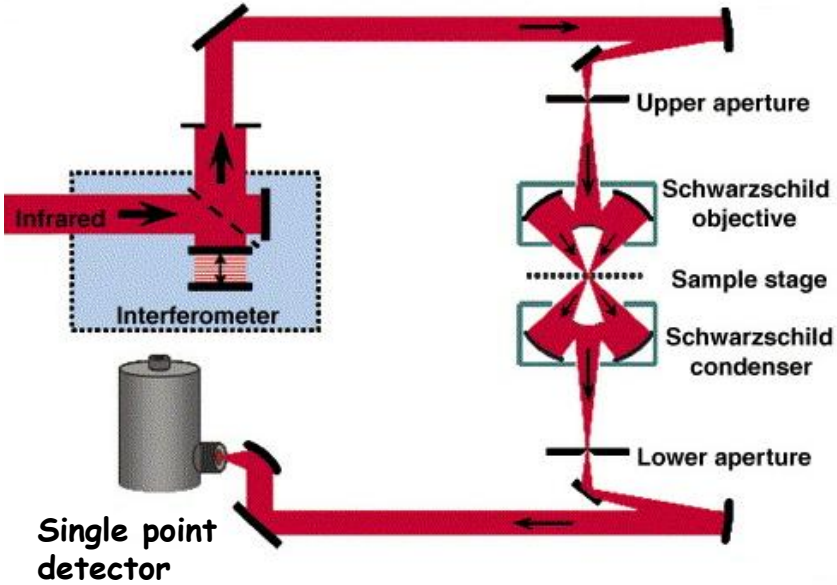

Optical sample image

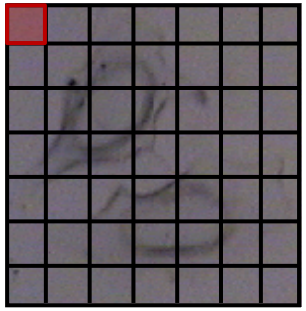

- The map pixel size is provided by the aperture settings
- Sequential acquisition: Slow imaging of large sample areas
- Low detector noise, high SNR

Chemical sample image

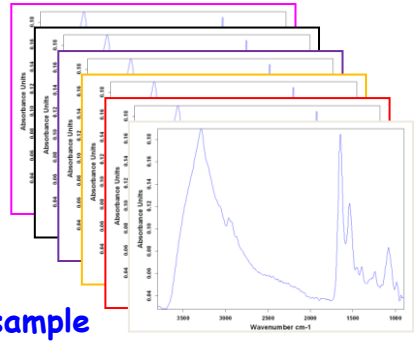

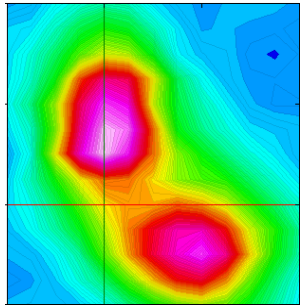

Imaging layout

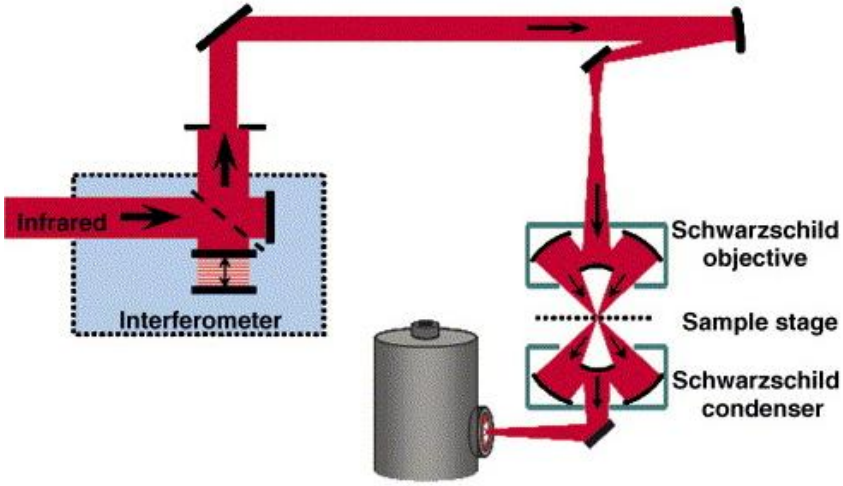

Optical sample image

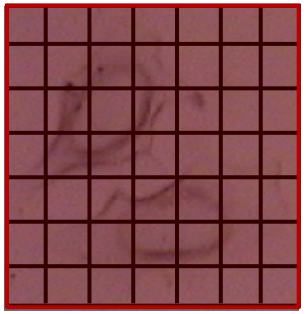

- The image pixel size is provided by the individual pixel of the detector
- Parallel acquisition: Fast imaging of large sample areas
- High detector noise, low SNR

Adapted from: L.Miller, P. Dumas, BBA 1758:846, 2006

InfraRed Synchrotron Radiation (IRSR) _ Sources

Standard Bending radiation

Emitted during the circular trajectory in the bending magnet (BM) due to the constant magnetic field, B

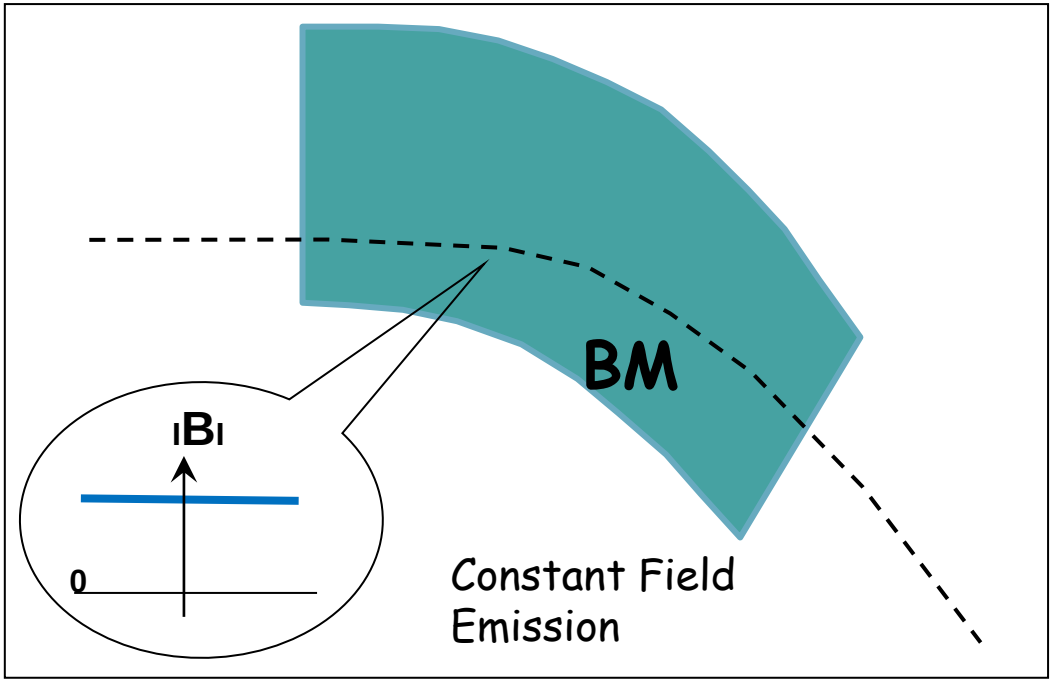

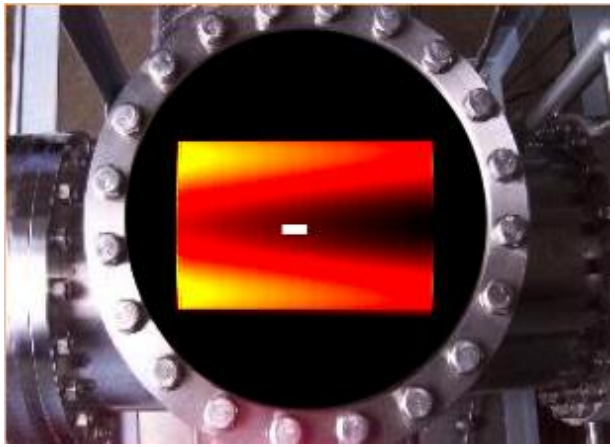

Natural opening angle

$$\Theta_{V\text{-}NAT}(\text{rad}) = 1.66\ (\lambda / \rho)^{1/3}$$

$$P\ (\lambda) = 4.4\ 10^{14} \times I \times \Theta_H \times bw \times (\rho/\lambda)^{1/3}\ \text{photons s}^{-1}$$

I (A) is the ring current, Θ_H **(rads)** the horizontal collection angle, ***bw*** **(%)** the bandwidth, **λ (μm)** the wavelength, and **ρ (m)** the radius of the bending

Edge Emission

Emitted at the entrance (exit) of a bending magnet due to the rapid variation of the B field

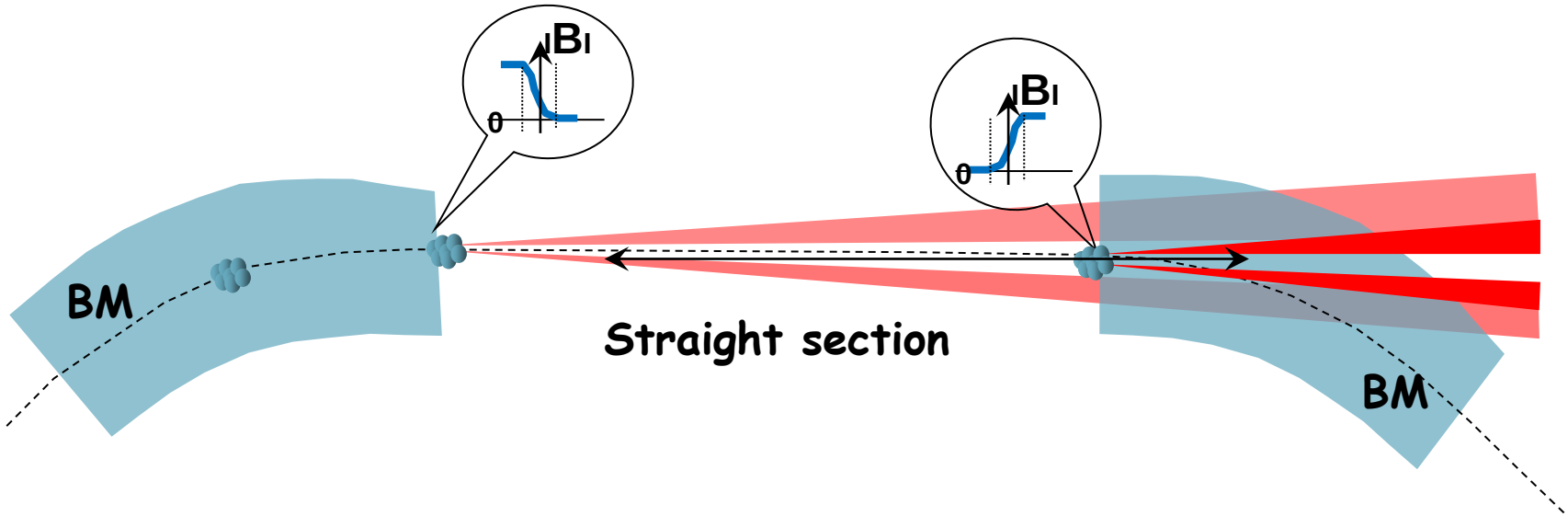

In the Far-Field approximation:

$$P = \alpha \times I \times \gamma^4 \Theta^2/(1+ \gamma^2 \Theta^2)^2 \text{ photons s}^{-1}$$

I is the current in amperes,
Θ (rads) the emission angle
(concentrated in $\Theta_{max} \sim 1/\gamma \sim 10$ mrads)

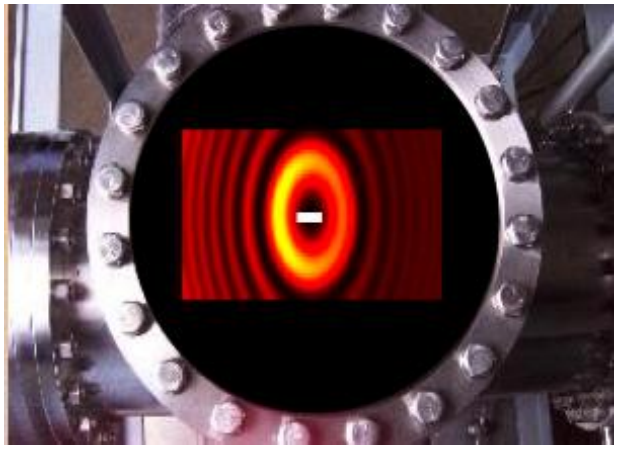

InfRared Synchrotron Radiation (IRSR) _ Characteristics

The IRSR Flux and Brilliance depend on:

- beam current
- source size/emittance
- extraction aperture
- transmission optics

Instead scarcely depend on the machine energy

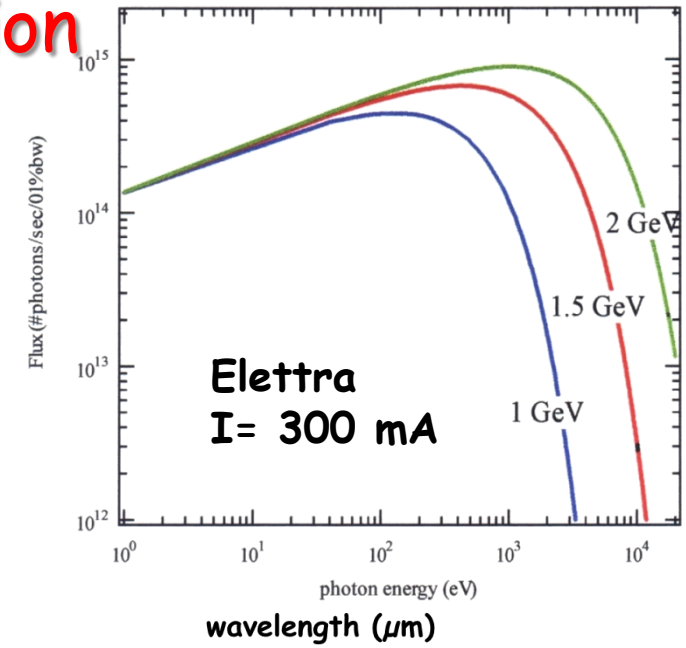

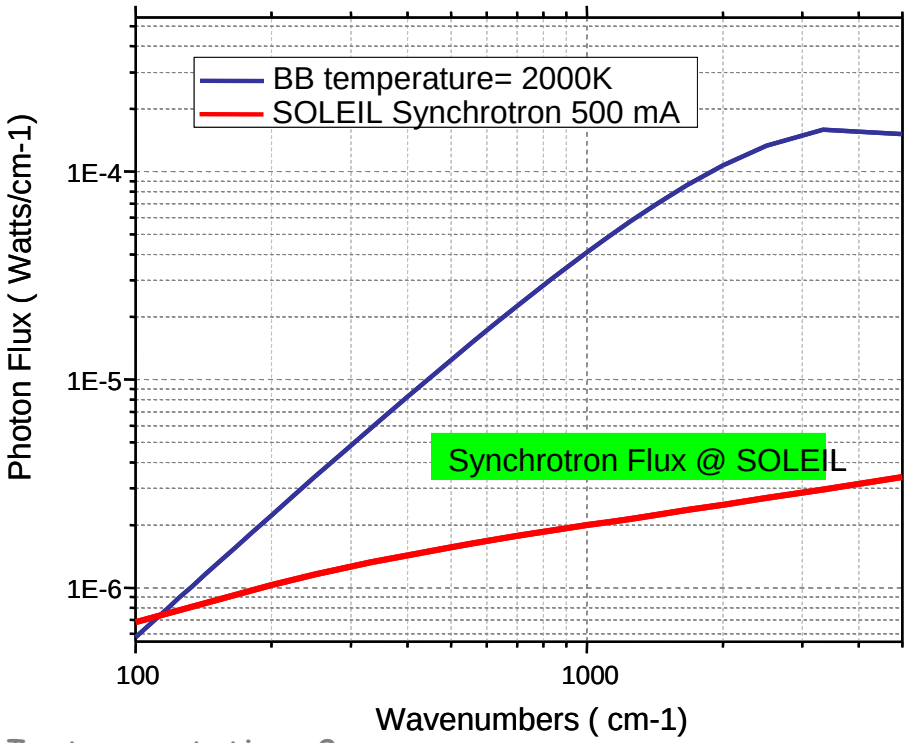

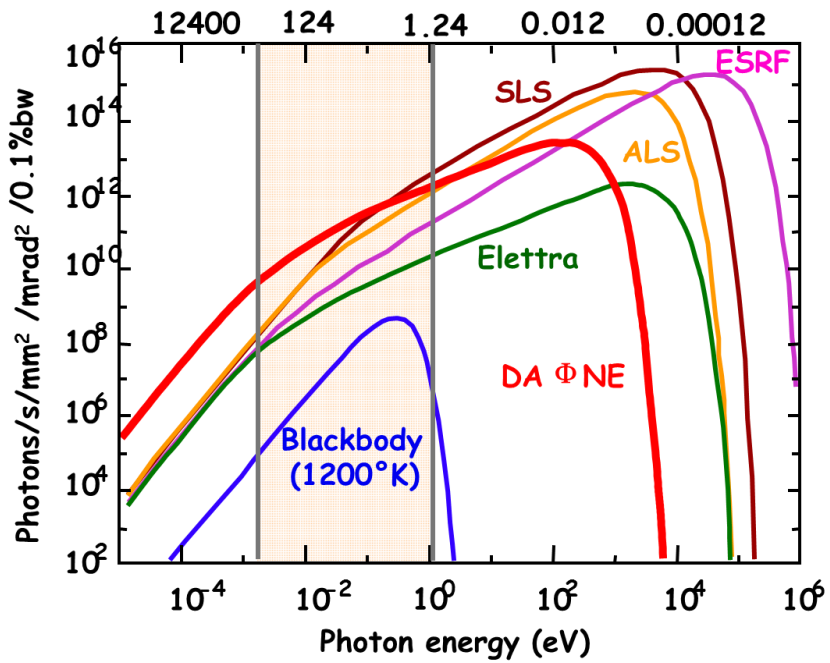

InfRared Synchrotron Radiation (IRSR) Advantages

BROADBAND

BRIGHTNESS

LINEAR & CIRCULAR POLARIZATION

PULSED EMISSION

Diffraction limited spatial resolution

Better Signal-to-Noise

Faster Data Collection

Spectroscopy

Microscopy

Polarized (micro)spectroscopy of oriented substrates

Time resolved studies

IR beamline design

Conventional IR beamline layout: SISSI@Elettra

Radiation is collected over a solid angle of
65 mrad (H) x 25 mrad (V)

M1 Plane mirror
M2 Ellipsoidal mirror
M3 Plane mirror
M4 Ellipsoidal mirror

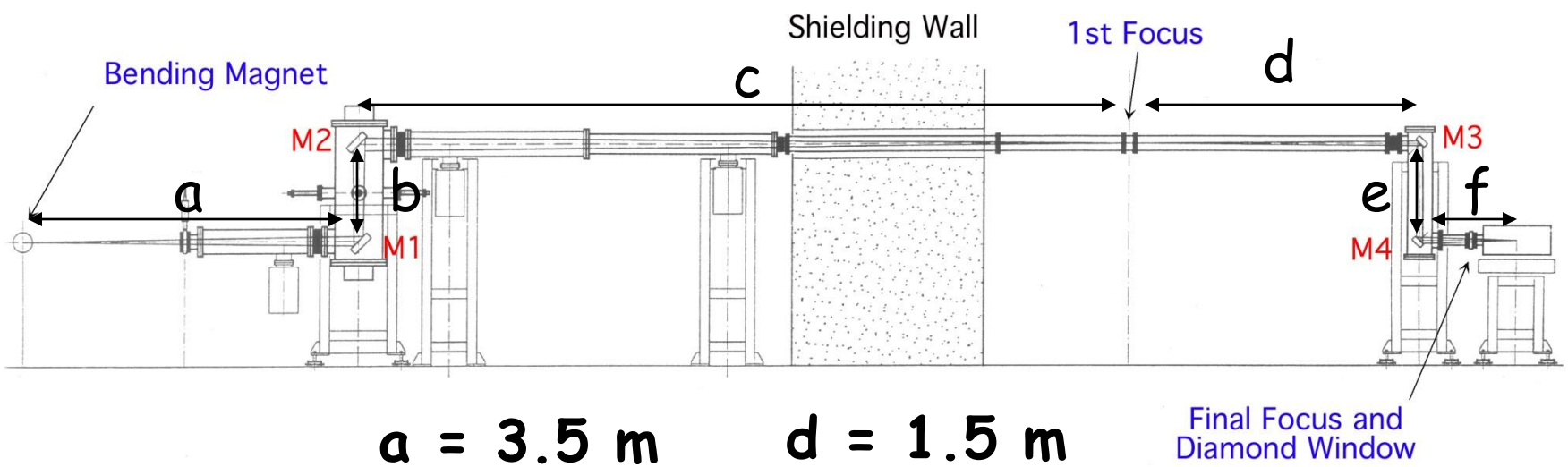

a = 3.5 m d = 1.5 m

b = 1.0 m e = 1.0 m

c = 11.5 m f = 2.5 m

SISSI first chamber

The water-cooled extraction mirror (M1)

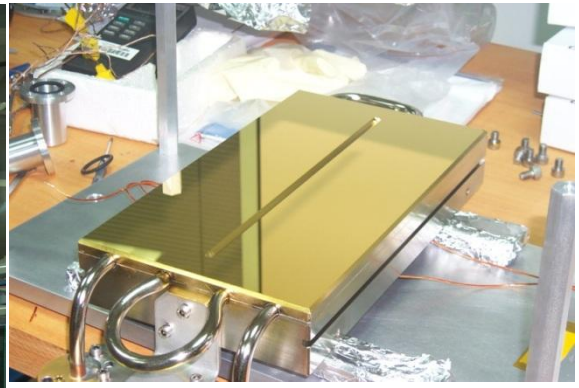

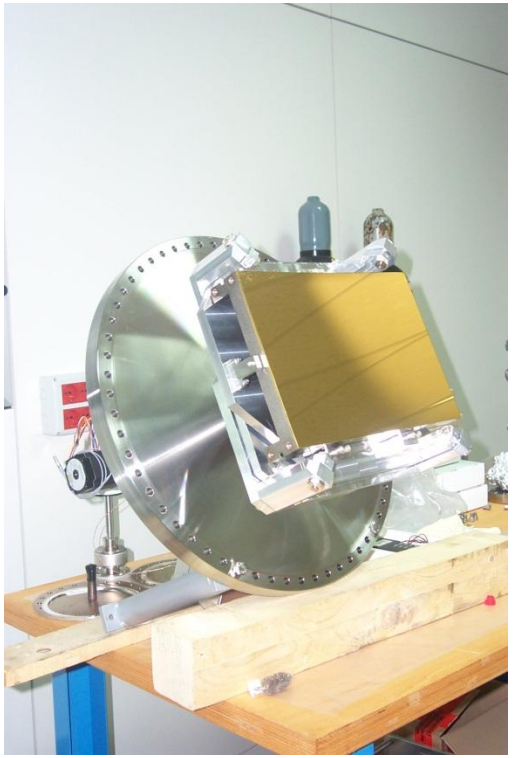

The focusing Ellipsoidal mirror (M2)

Intensity distribution on the extraction mirror (photons*0.1%bw/mm^2)

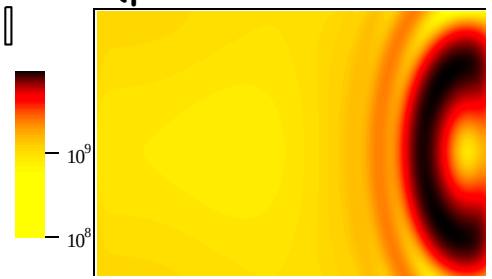

10 meV
~ 80 cm^{-1}

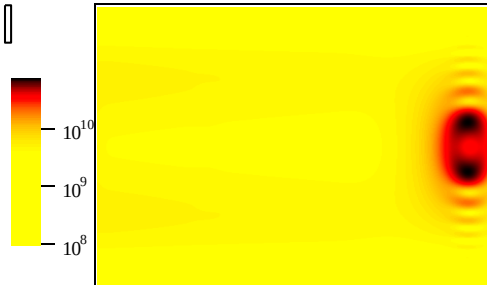

100 meV
~ 805 cm^{-1}

500 meV
~ 4000 cm^{-1}

1 eV
~ 8000 cm^{-1}

MIR performances of SISSI@Elettra

Diffraction-limited lateral resolution is practically achievable only by exploiting the brightness advantage of SR

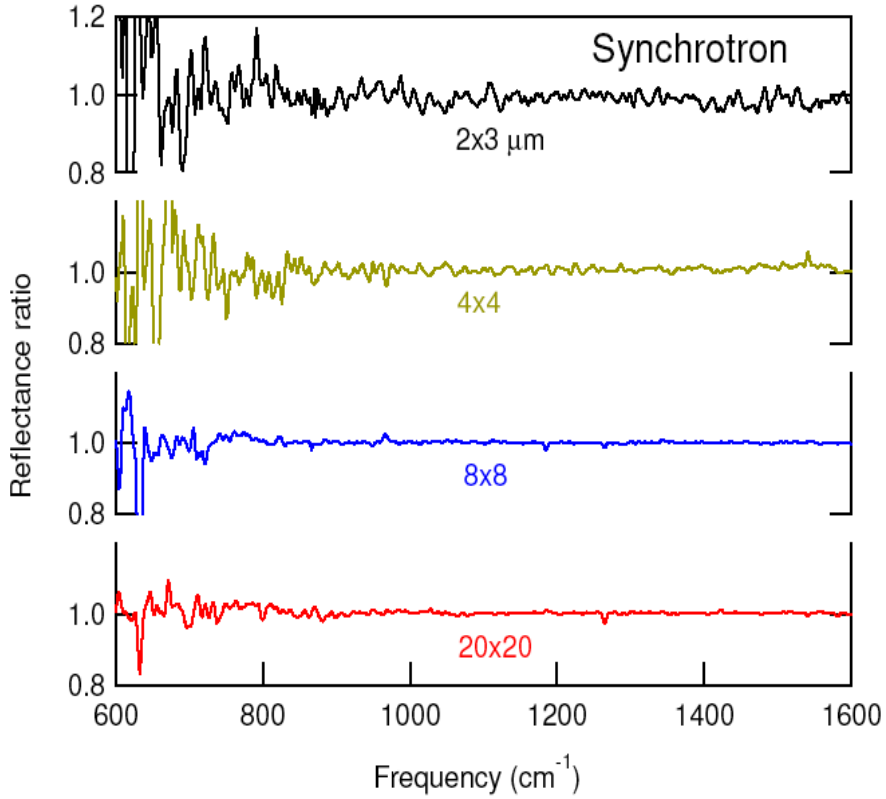

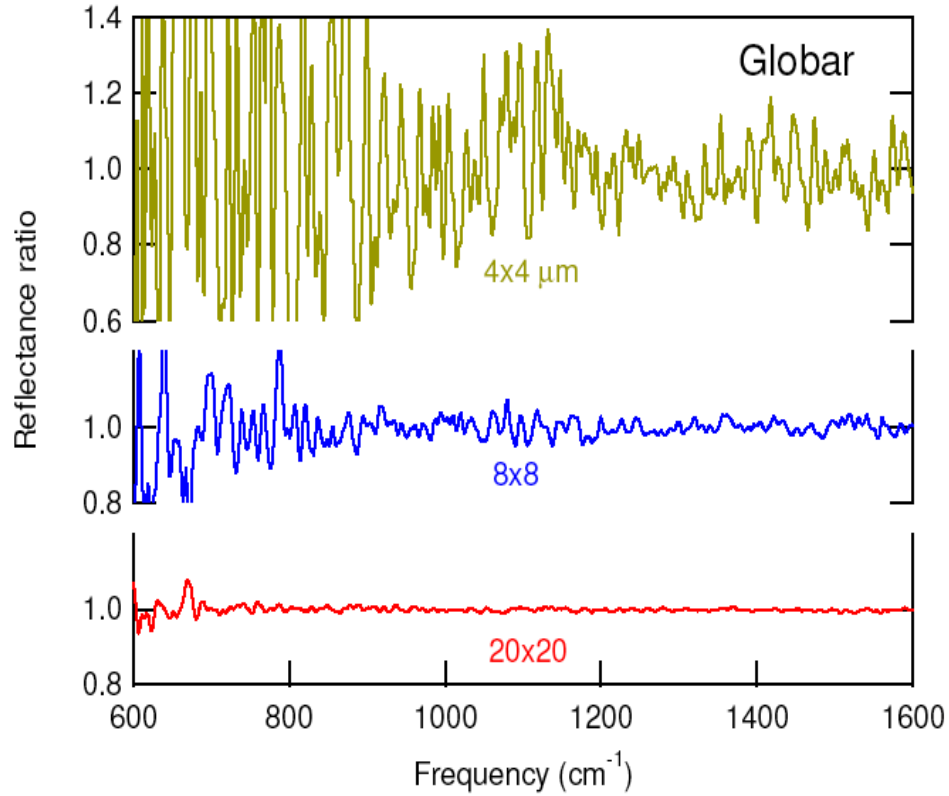

N_2 cooled MCT detector, 128 scans, 4 cm^{-1} spectral resolution

Figure of merit of SISSI@Elettra

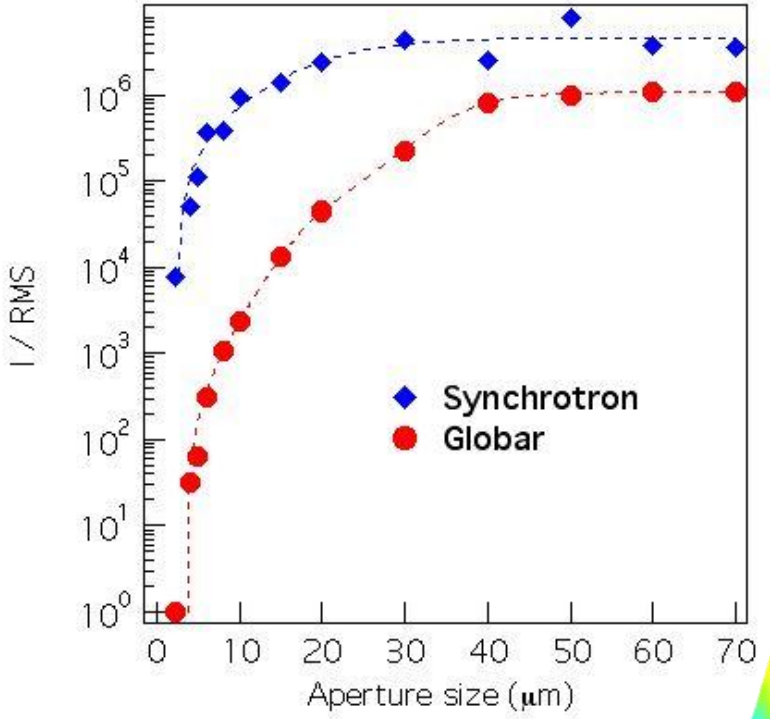

MIR
MCT detector, 128 scans, 4 cm^{-1}

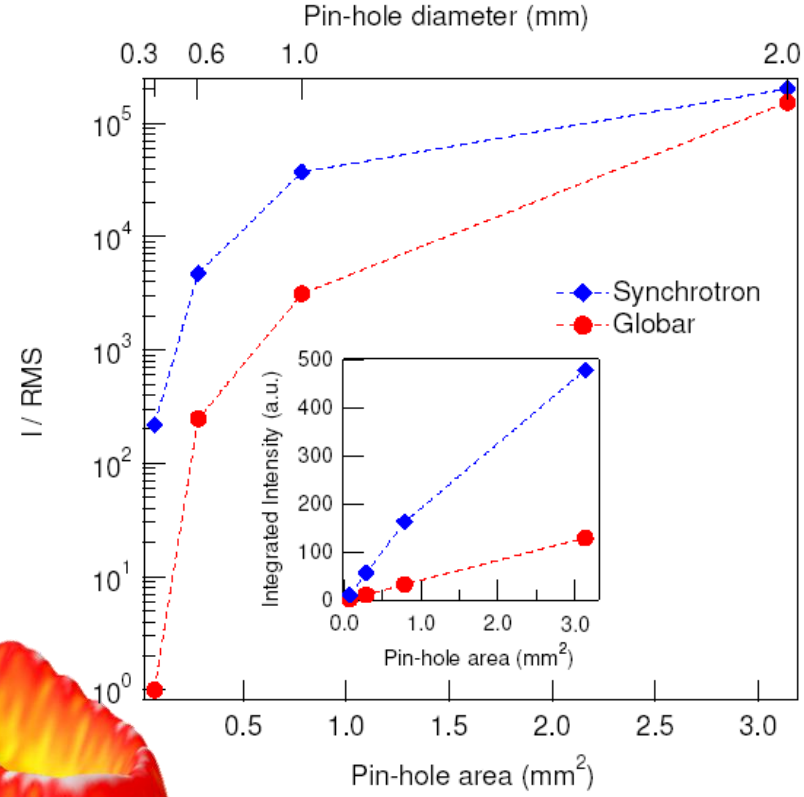

FIR
Si bolometer, 128 scans, 4 cm^{-1}

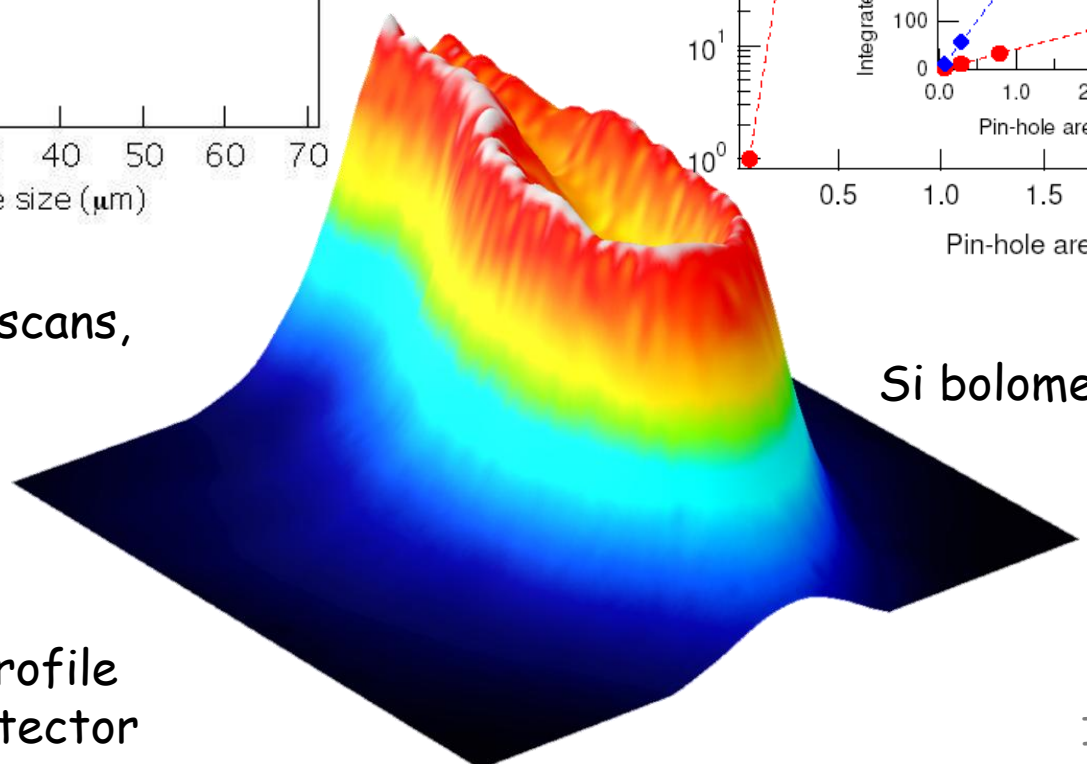

SISSI MIR beam profile imaged with FPA detector

Beamline branches simultaneously working

At SISSI beamline, the two branches can not operate simultaneously

More recent beamlines in newer 3rd generation SR facilities split BM and ER contributions for the simultaneous operation of two branches

SMIS @ Soleil

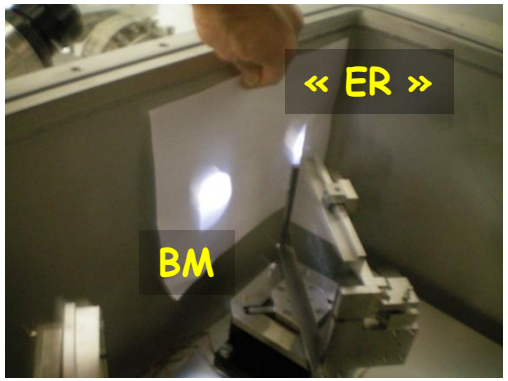

Microscope 2
Branche ER

Microscope 1
Branche BM

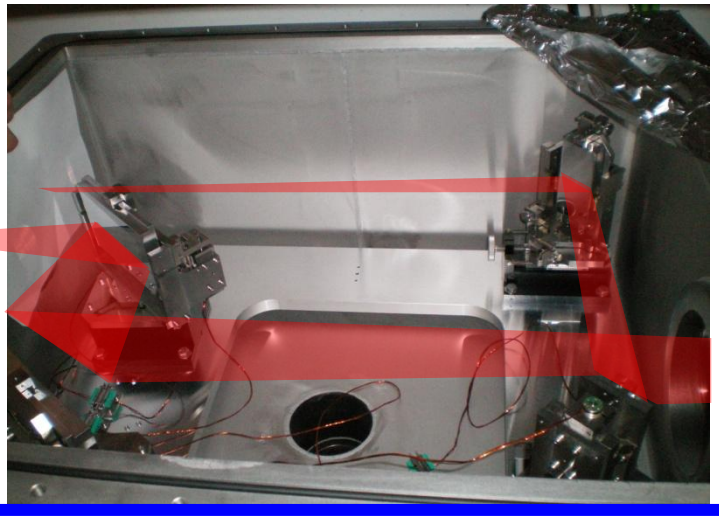

More recent IR beamline layout: IRENI@Synchrotron Radiation Center, Wisconsin-Madison

The FTIR imaging approach: fast acquisition speed

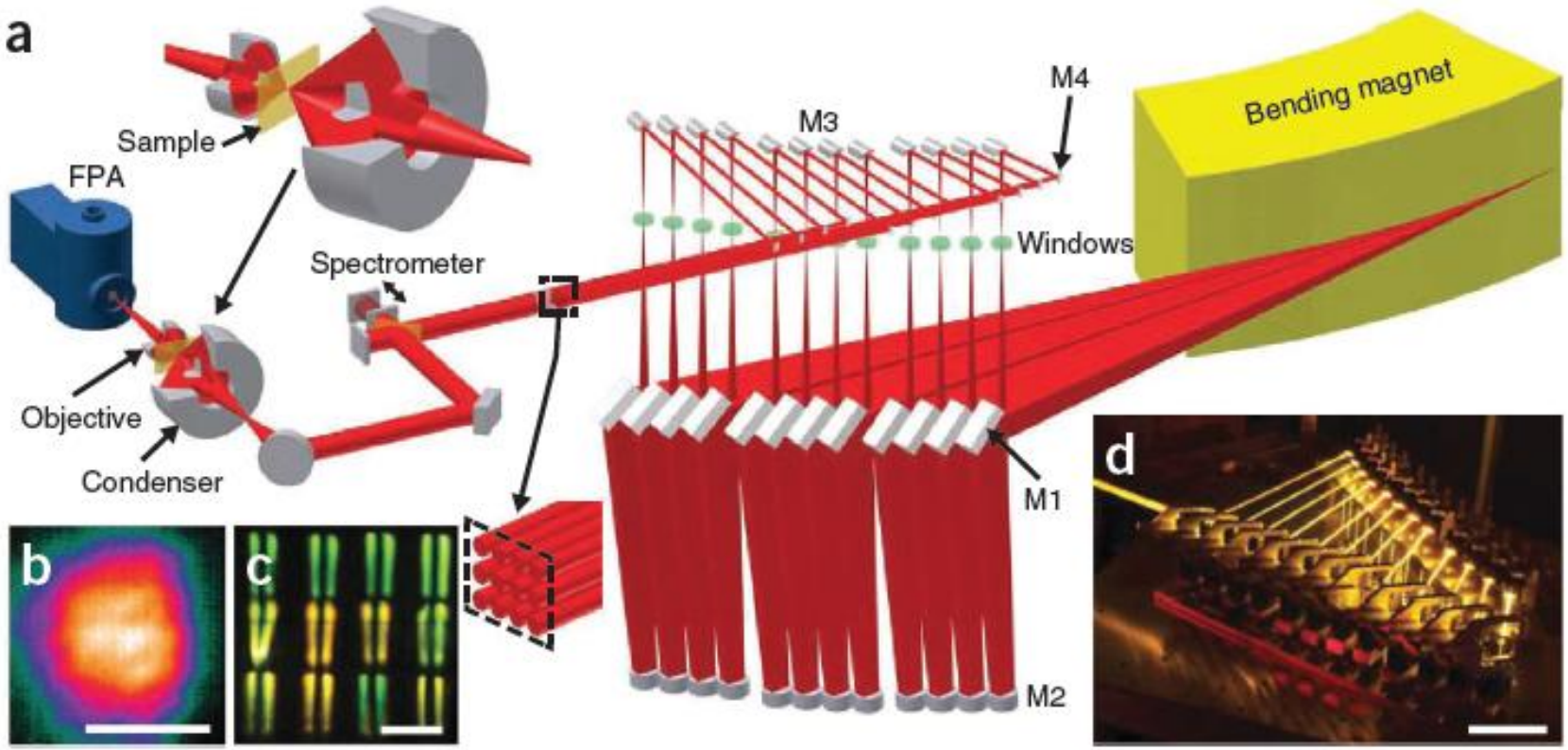

From M.J. Nasse *et al.*, Nature methods, 8:413 (2011)

IRSR Beamlines in the World

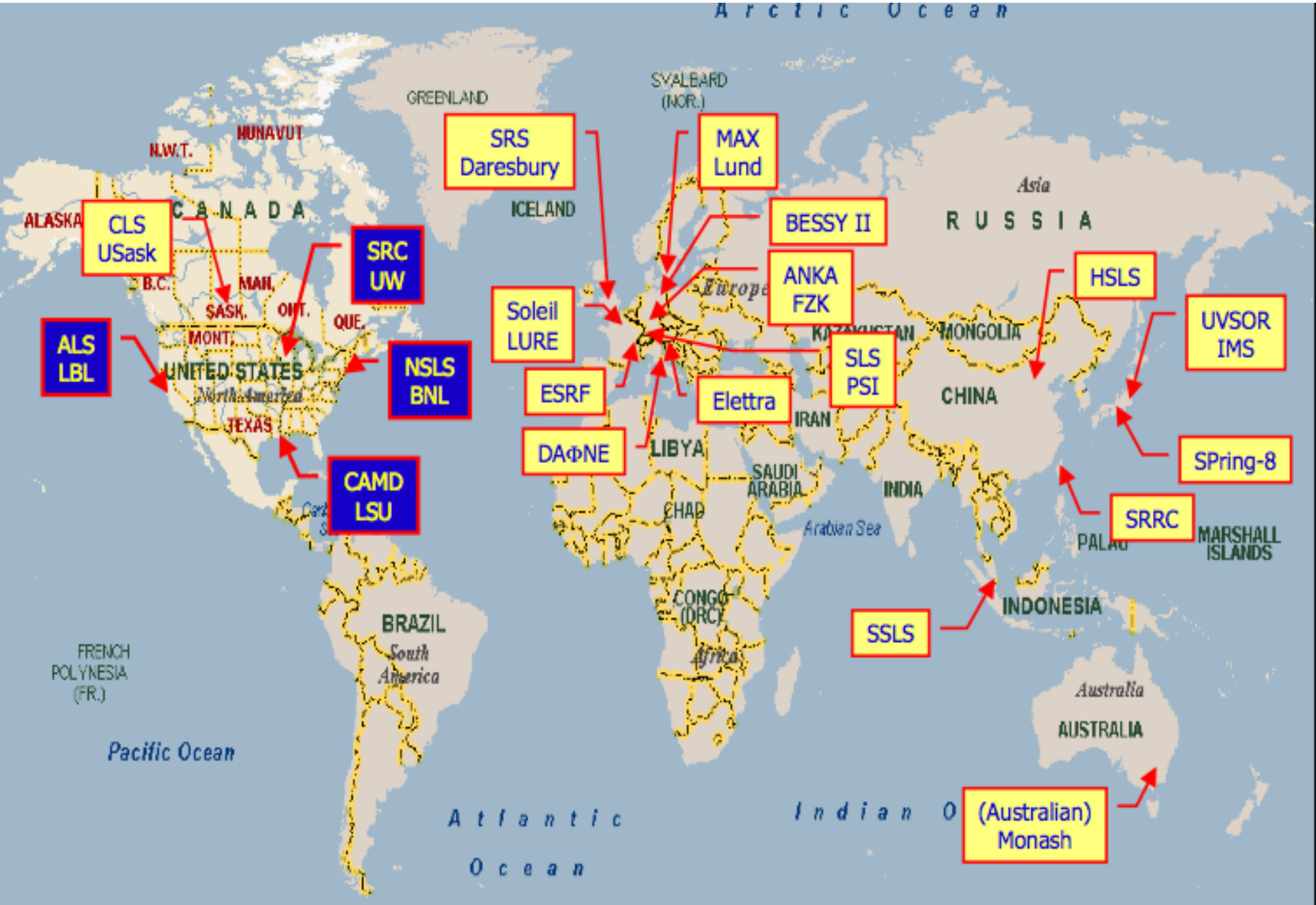

FTIR spectroscopy for environmental sciences

- Bacteria and biofilm characterization
- Transmissible spongiform encephalopathies
- From wood to biofuel

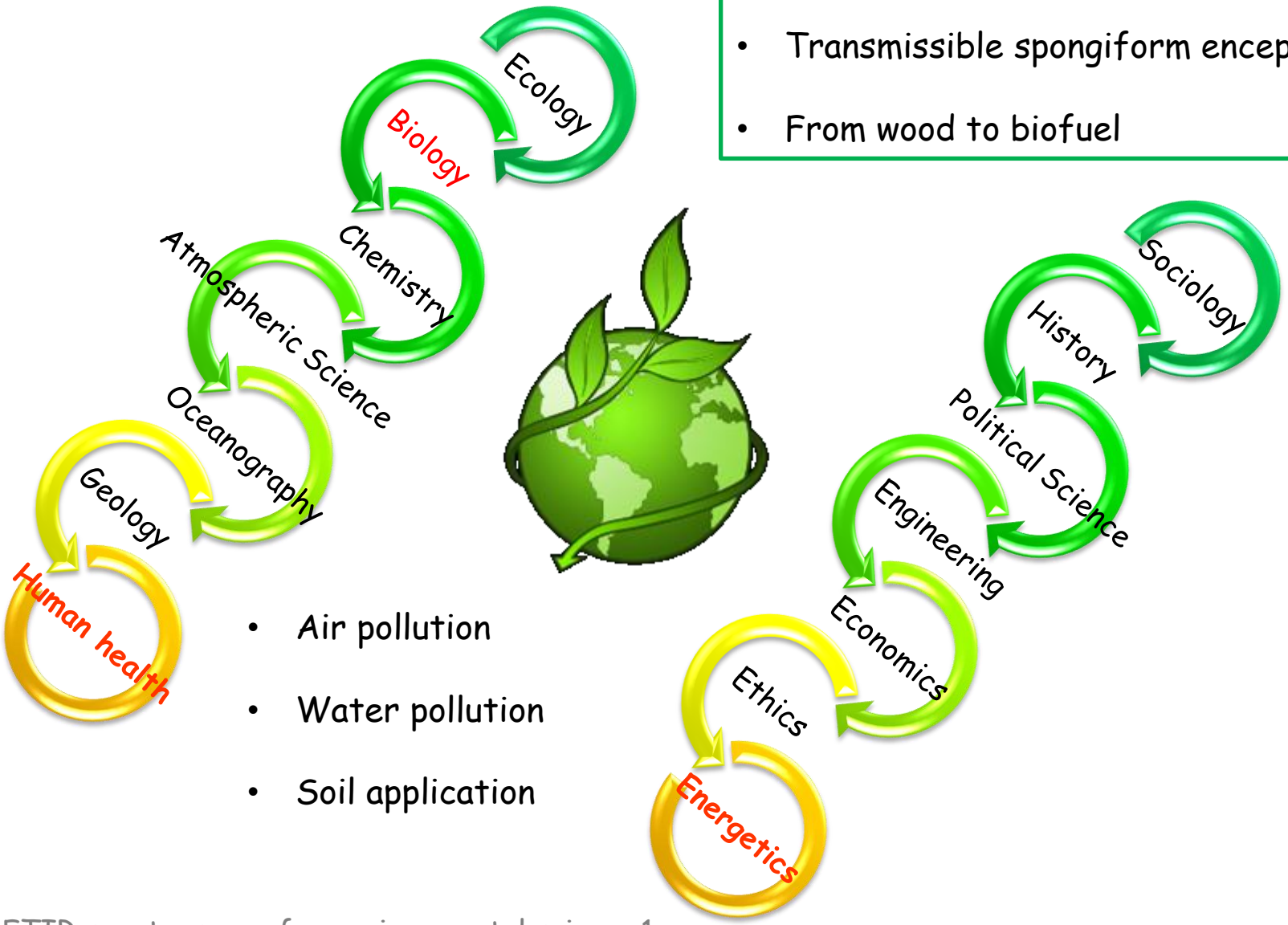

- Air pollution
- Water pollution
- Soil application

Biology:
The spectroscopic point of view

Biology is the branch of natural science that studies life and living organisms.

The building blocks of life are the **cells**

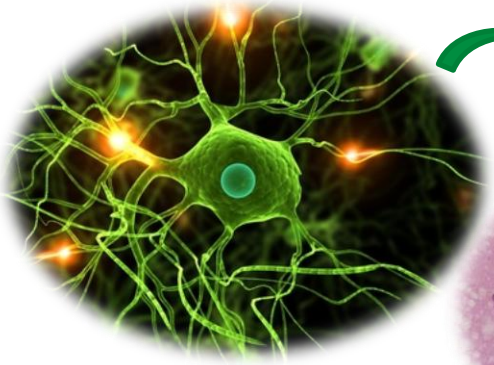

Cell

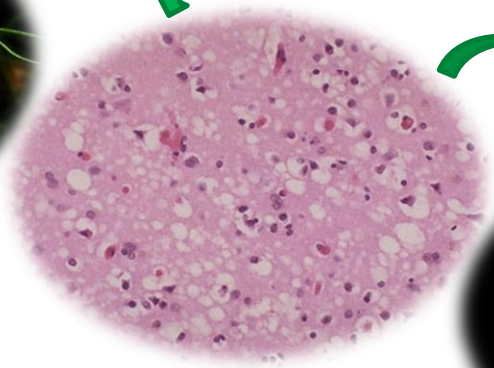

Tissue

Organ

Organism

The study of the chemical processes in living organisms is the subject of **Biochemistry**

It deals with the <u>structures</u> and <u>functions</u> of cellular components such as **proteins**, **carbohydrates**, **lipids**, **nucleic acids** and other **biomolecules**

The cellular architecture
Prokaryotic versus Eukaryotic
mammalian versus vegetal

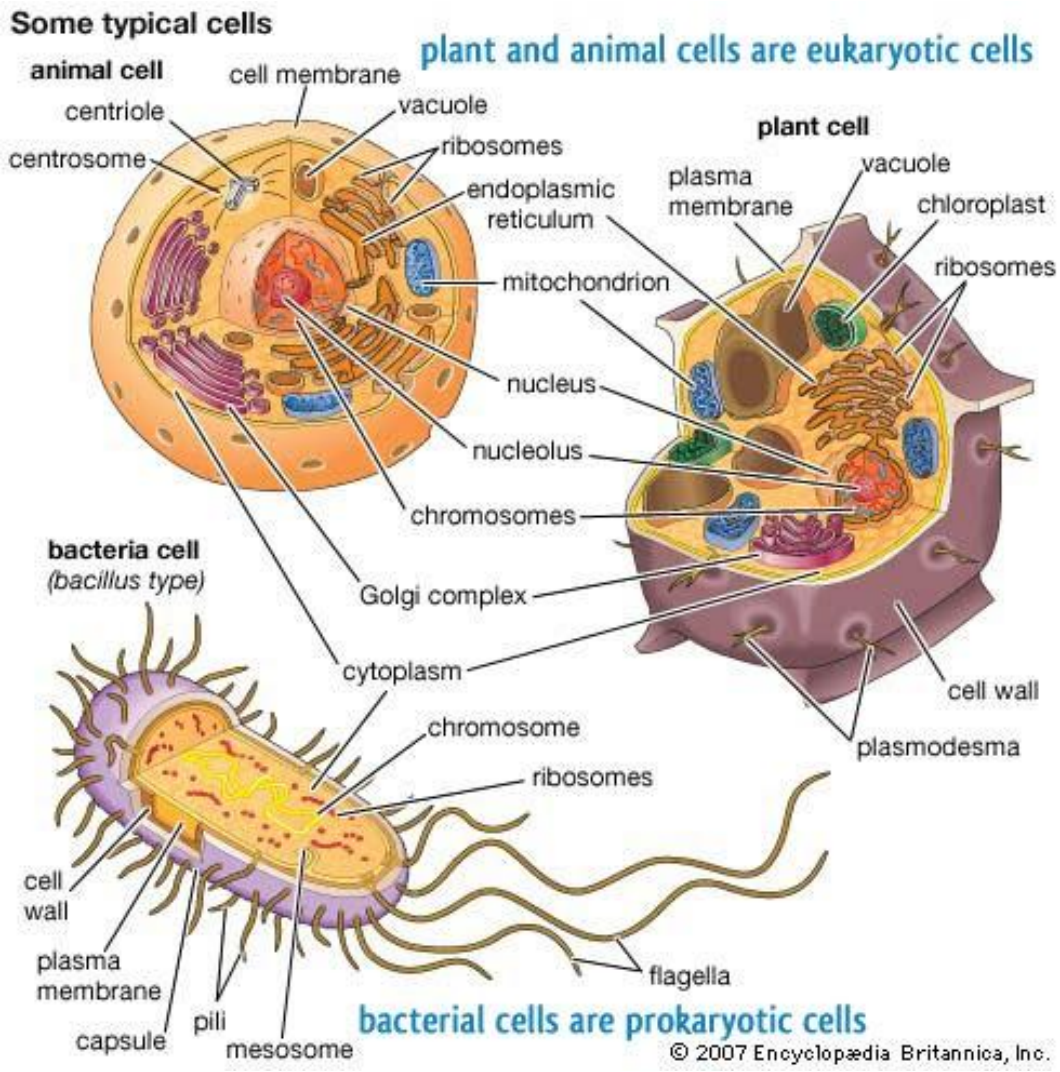

The eukaryotic/prokaryotic cell spectrum

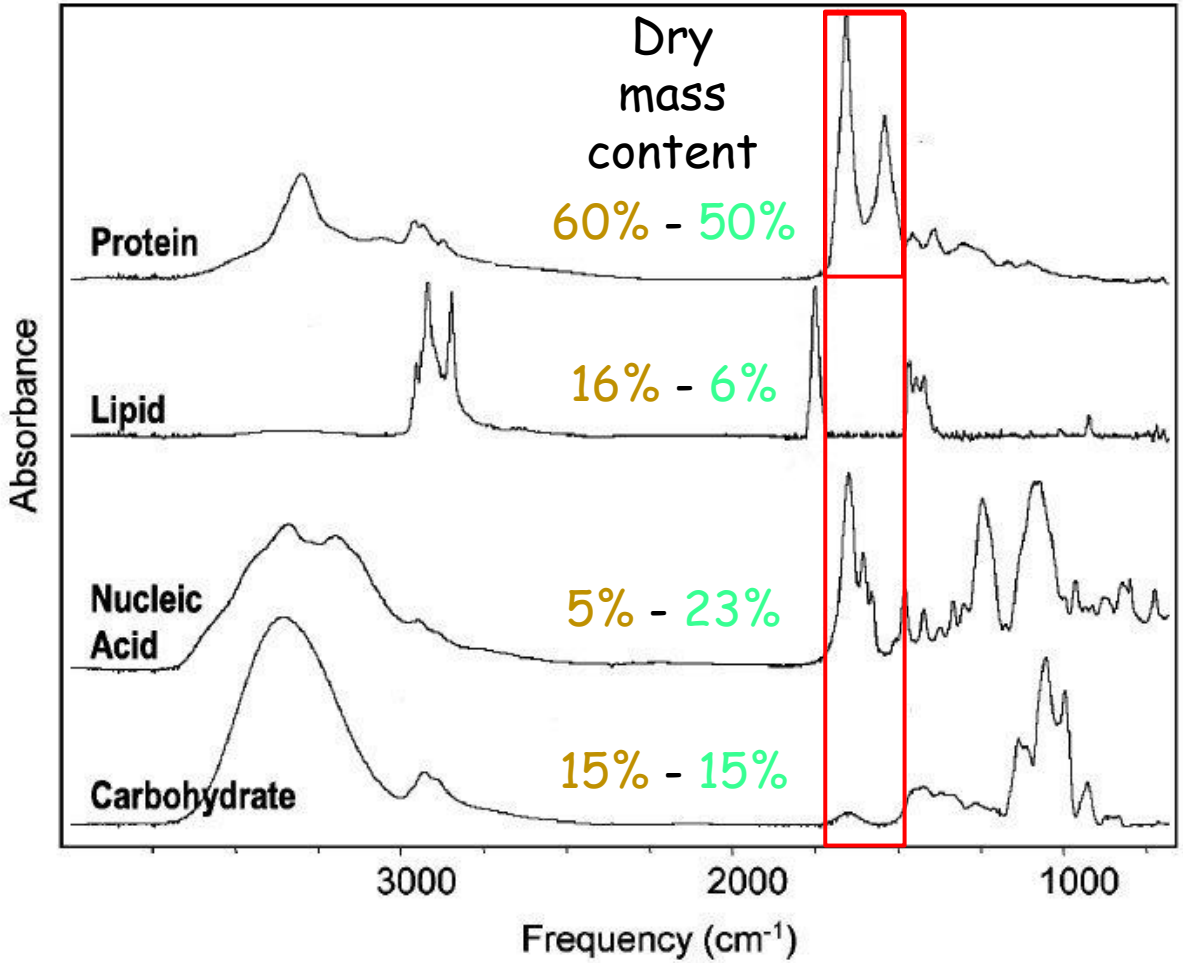

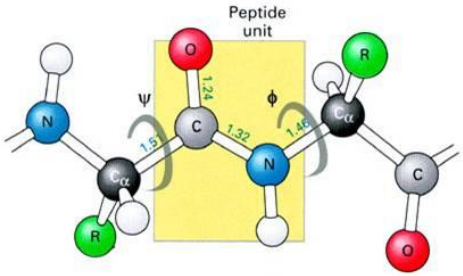

1700-1600

1705-1690 : ν C=O RNA

1660-1650 : ν C=O DNA

1660-1650 : ν C=O RNA

1700-1600: Amide I

80% ν C=O + 10% ν C-N +10% δ N-H

1600-1500

1600-1500: Amide II

40% ν C-N + 60% δ N-H

Adapted from: L. M. Miller, G.D. Smith and G. L. Carr, *Journal of Biological Physics*, 29 (2-3), 219-230, **2003**

The eukaryotic cell spectrum

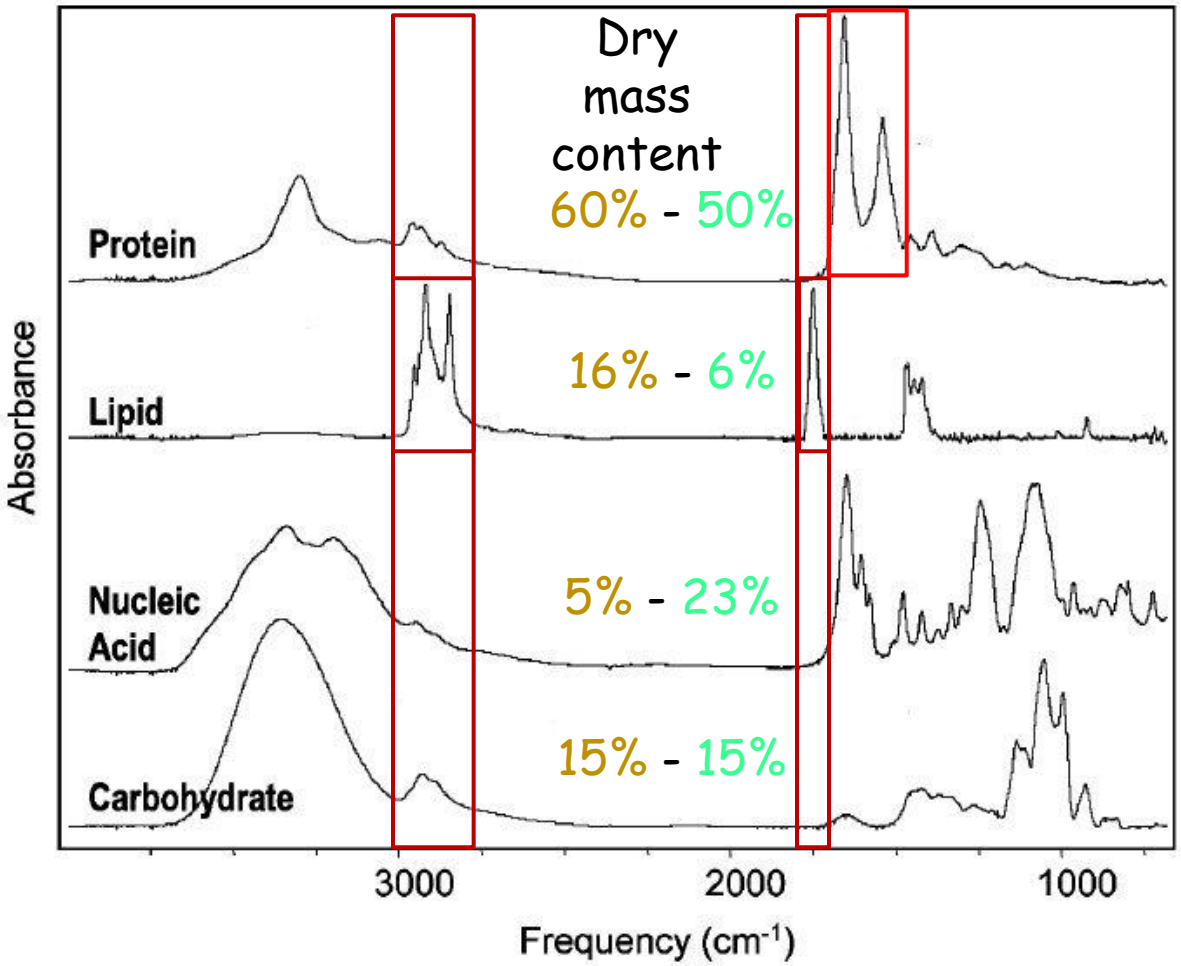

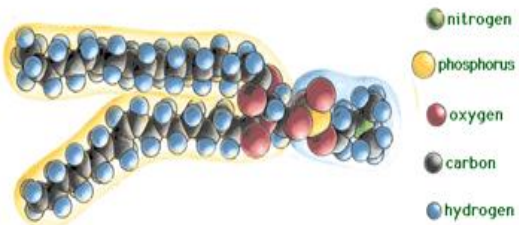

Saturated Acyl chains

2950-2960 : ν_{as} (CH_3)

2915-2925 : ν_{as} (CH_2)

2867-1877 : ν_s (CH_3)

2845-2855 : ν_s (CH_2)

Unsaturated Acyl chains

> 3000 : ν (=CH)

Ester Band

1700-1750 : ν (C=O)

The eukaryotic cell spectrum

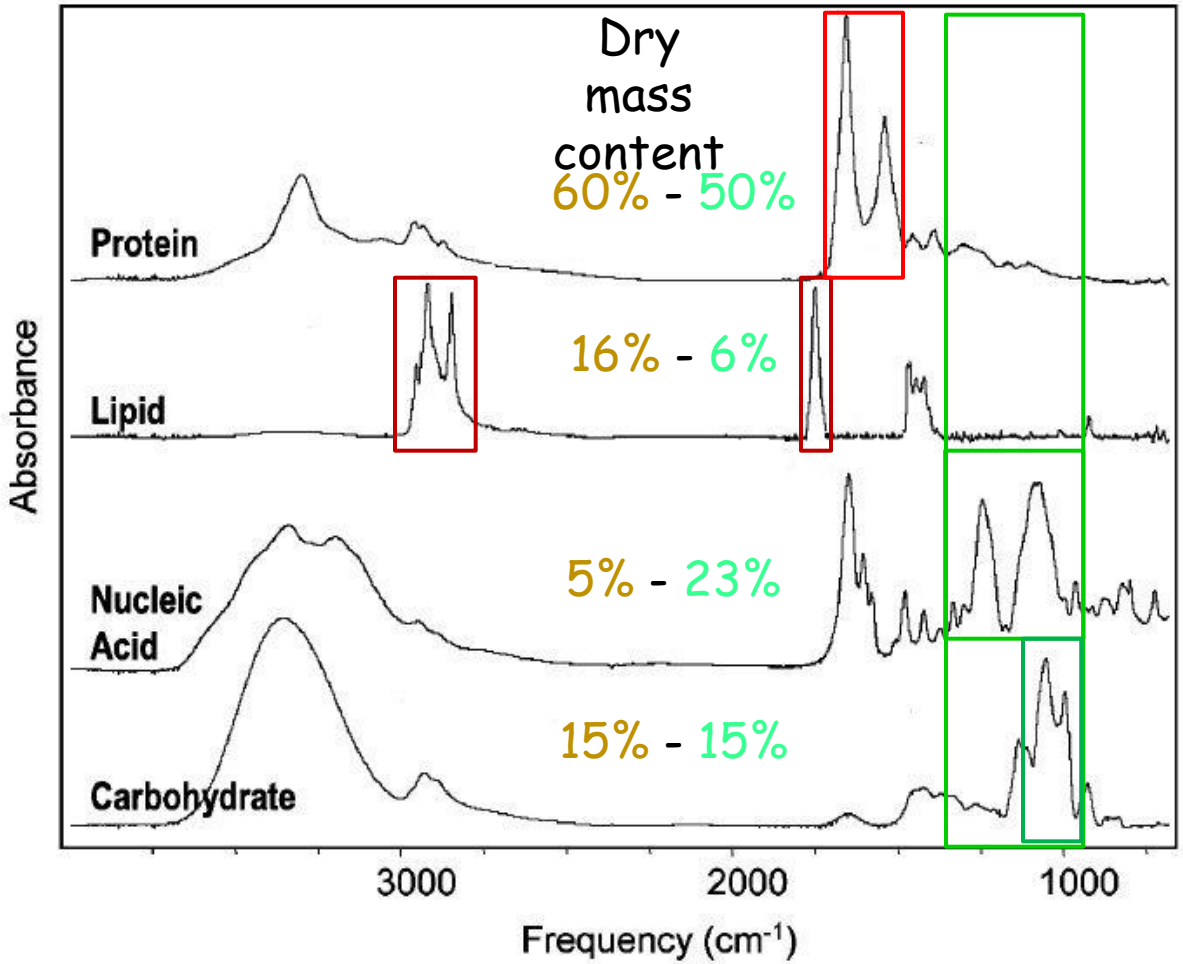

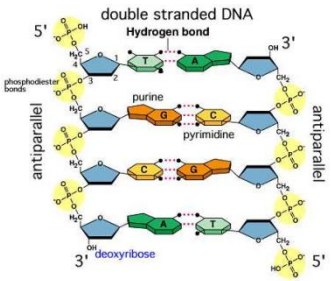

1250-1200

1244 : ν_{as} PO^{2-} RNA

1230 : ν_{as} PO^{2-} DNA

1100-1050

1089 : ν_{s} PO^{2-} DNA

1084 : ν_{s} PO^{2-} RNA

1100-1000

DNA and RNA ribose

ν C-O

Complex network of carbohydrate bands

The eukaryotic cell spectrum

Band intensity, position, width and shape (band components) are sensitive to subtle biochemical changes of bio-specimens.

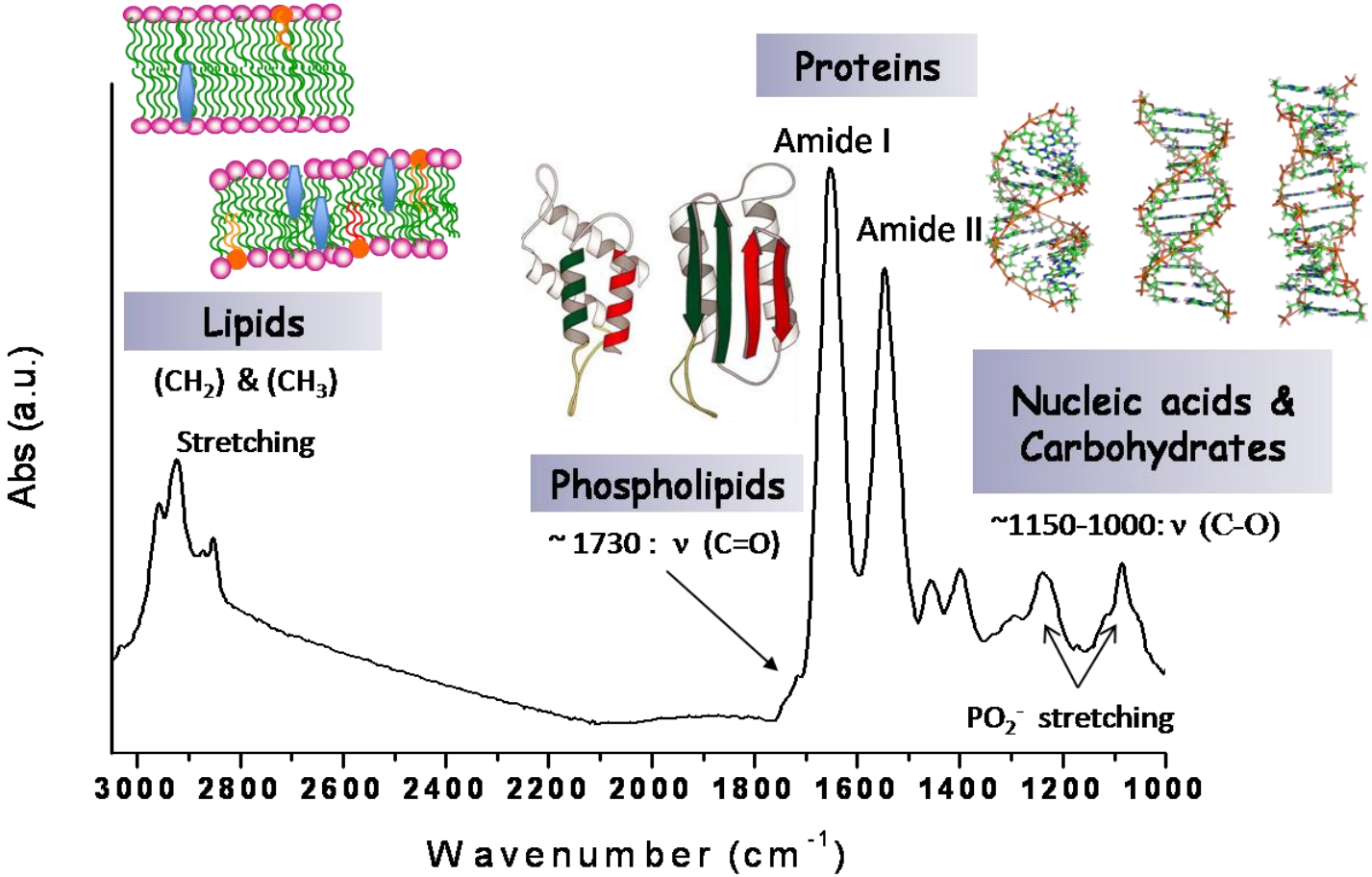

Compositional and structural information at tissue, cellular and sub-cellular level can be achieved by exploiting SR brightness advantage

From the sample to the biological information

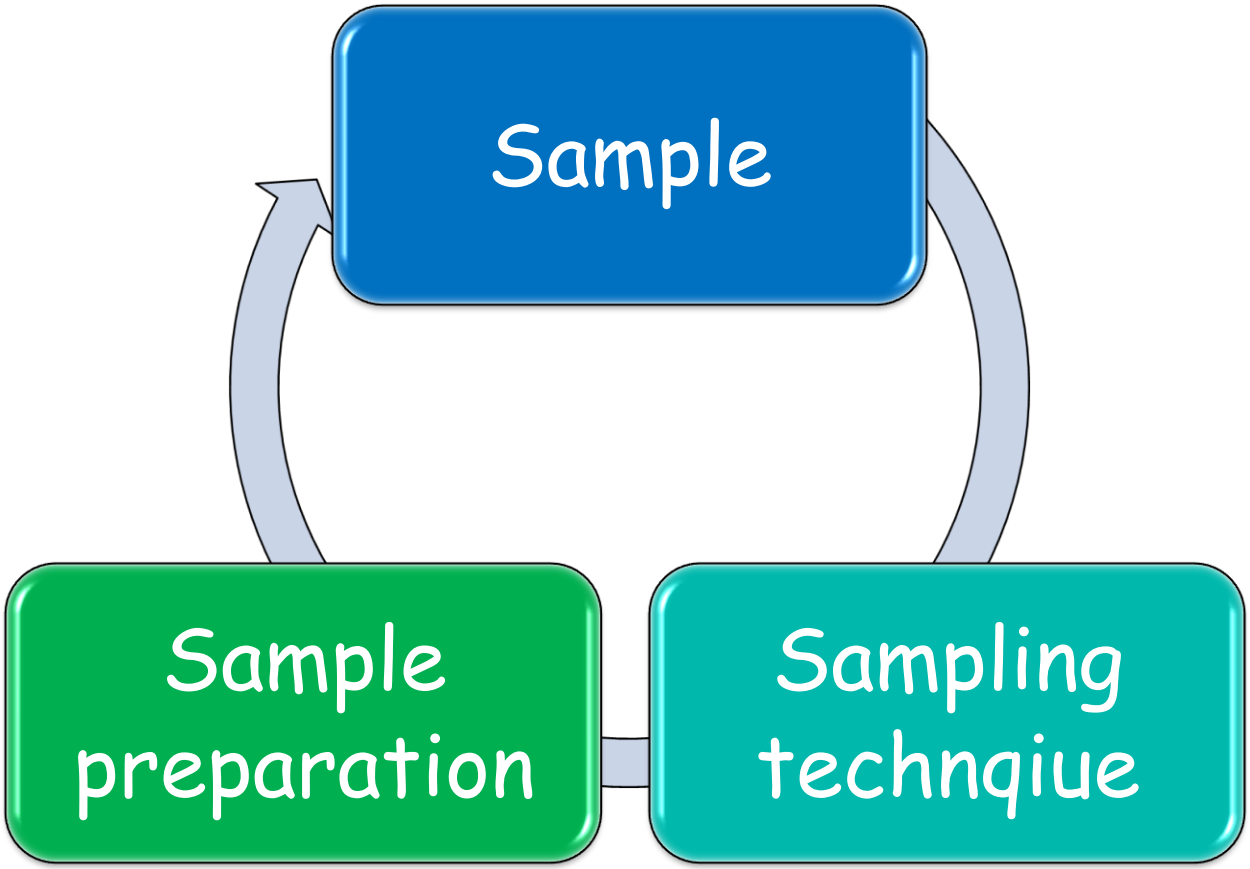

Sampling techniques

- TRANSMISSION

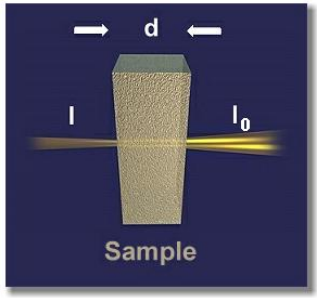

The **absorption** behavior of the entire sample is investigated

- TRANSFLECTION

- REFLEXION

  - SPECULAR

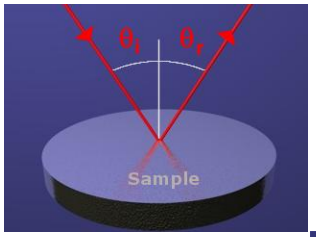

Typical angle of incidence = 10-30°
The **reflection** behavior of the bulk sample is investigated

  - GRAZING INCIDENCE

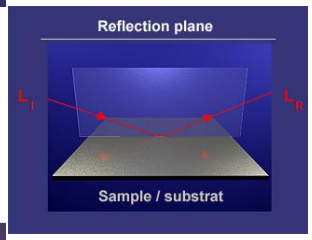

Typical angle of incidence = 50-85°
The **surface properties** of the sample are investigated

  - DIFFUSIVE

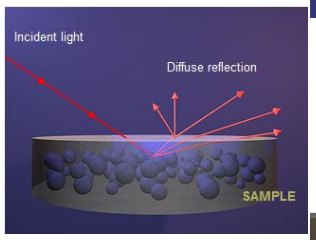

The diffusive-reflection spectrum is defined by the **absorption-scattering** behavior of the sample

  - TOTAL (ATR)

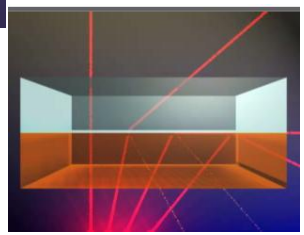

The **absorption** behavior of the sample surface in contact with the IRE is investigated

Transmission

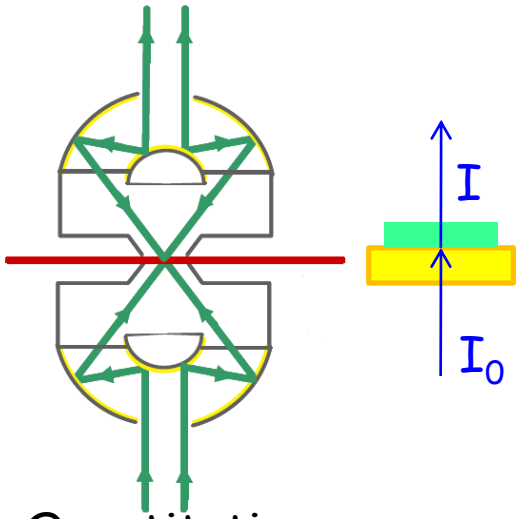

+ Quantitative

Lambert-Beer Law

$$A = -\log_{10}(I/I_0) = \varepsilon dc$$

$$[\varepsilon] = L \cdot mol^{-1} \cdot cm^{-1}$$

$$[c] = mol \cdot L^{-1}, [d] = cm$$

- Thin samples
  - Limited penetration depth
- Substrate materials must be IR transparent → expensive

Transflection

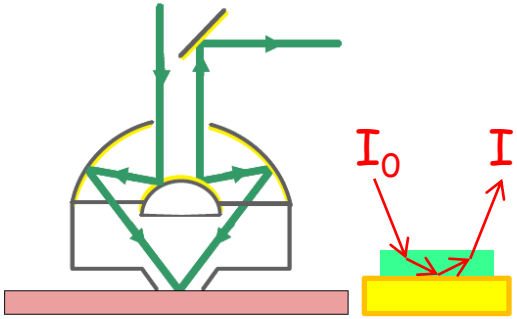

+ Substrate materials must be IR reflective → cheap
+ Improved absorbance signal

- Non quantitative
  - Electric field standing wave
- Thin samples
  - Limited penetration depth

ATR

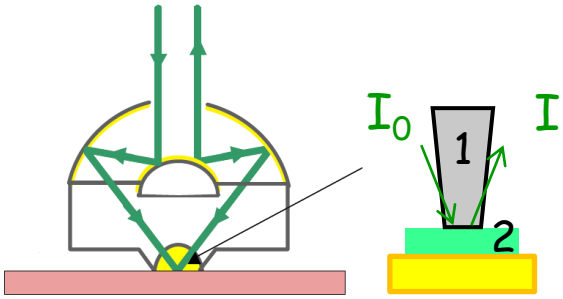

+ Surface sensitive technique

$$dp\ (penetration\ depth) = \frac{\lambda}{2\pi n_1 \sqrt{\left(\sin^2\theta - n_{2/1}{}^2\right)}}$$

+ Substrate "unaffected"

+ Sample thickness "unaffected"
- The absorbance is a function of λ and $n_{2/1}=n_2/n_1$

IR substrates

Sampling technique	Material	Vis-Transparent	MIR-Transparent	MIR-Reflective	Biocompa-tible	Other
Transflection	MirrIR-slides	Berely	No	Totally	Yes	Cheap +
Both	Si, Ge	No	Partially	Partially	Yes	Cheap
Transmission	Diamond	Yes	Partially	No	Yes	Expensive +
	BaF_2	Yes	Totally	No	No	Expensive
	CaF_2	Yes	Partially	No	Possibly	Expensive
	ZnSe	Slightly	Partially	No	No	Expensive
	Si_3N_4	Slightly	Partially	No	Yes	Fragile
	TEM grids	Yes	Totally	No	Yes	Fragile

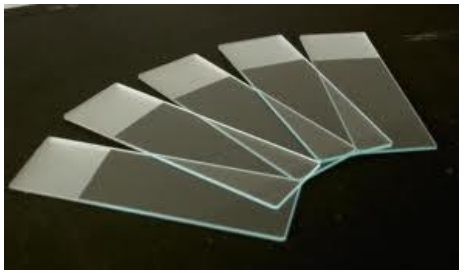

MirrIR slides

Si windows

ZnSe windows

CaF_2 windows

TEM grids

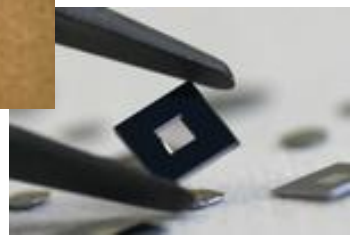

Silicon nitride windows

Electrical field standing waves

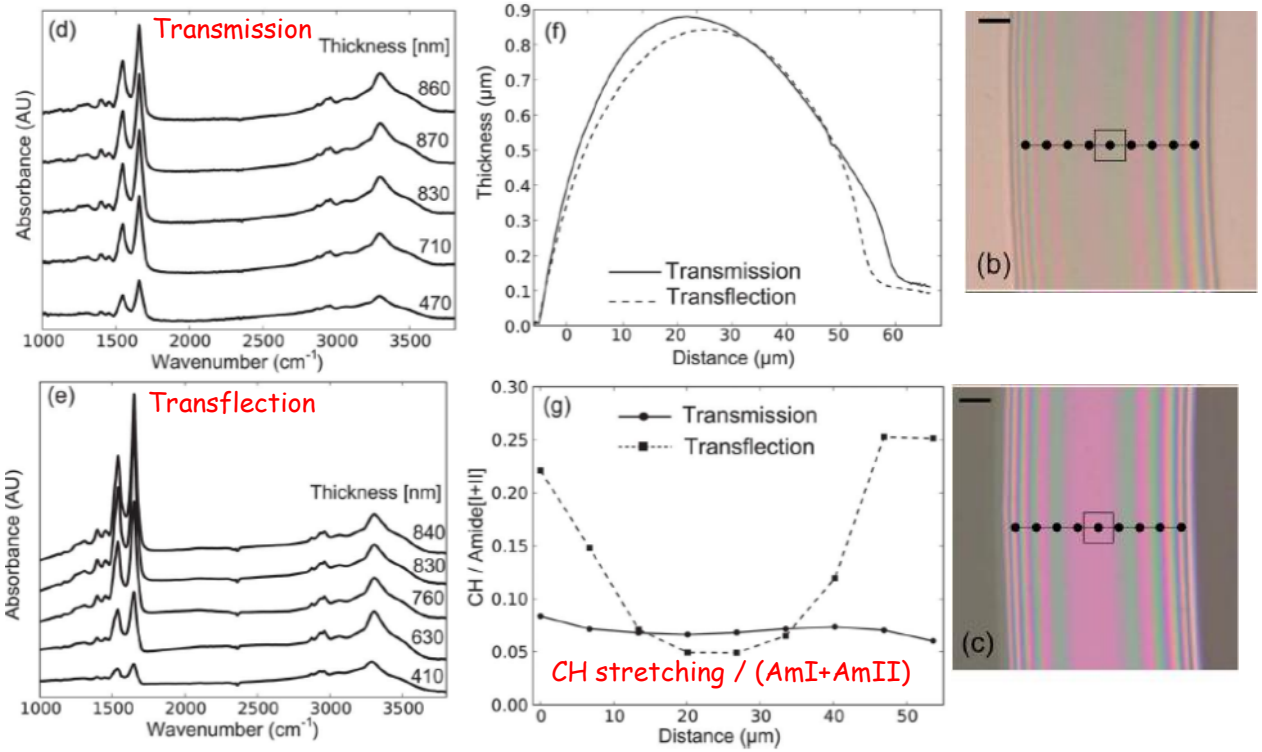

Adapted from: Jacob Filik , Mark D. Frogley , et al., Analyst, 2012, 137, 853-861

Curved films of BSA (Bovine Serum Albumin) protein have been measured at different profile points in transmission and transflection modes.

Transmission spectra behave as predicted by the Lambert-Beer law while tranflectance spectra do not.

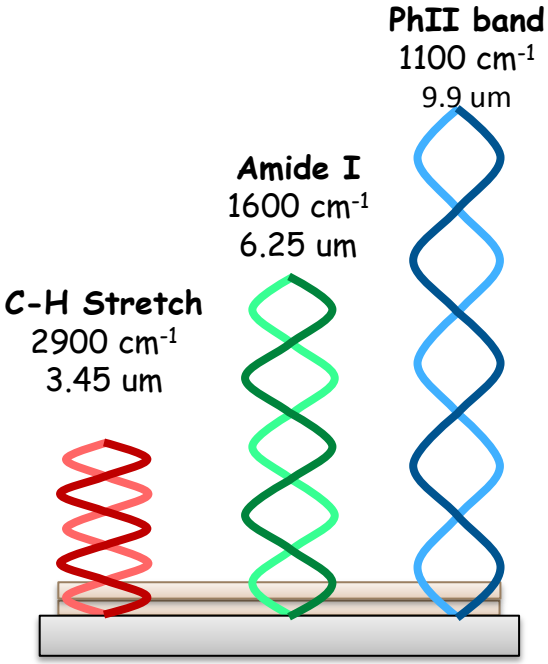

- Reflection from a metallic surface induces ~180° phase shifts of the electric field
- Incident and reflected waves interfere each other → electric field standing waves
- Node (destructive interference) and antinode positions (constructive interference) depend on the wavelength (stated constatnt refractive indexes of substrate, sample and surrounding medium)
- This caused relative band intensity changes with thickness

See also: Paul Bassan, Joe Lee, et al., Analyst, 2013, 138, 144-157

Sample preparation

Plant leave

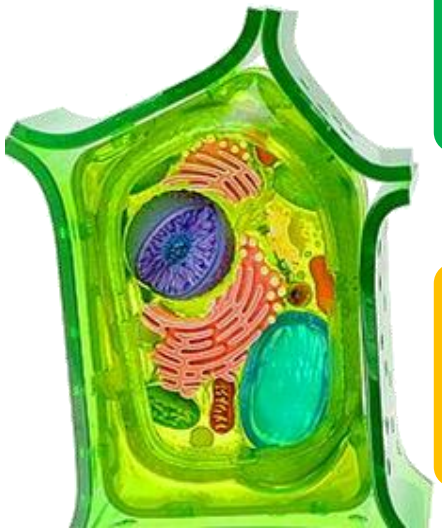

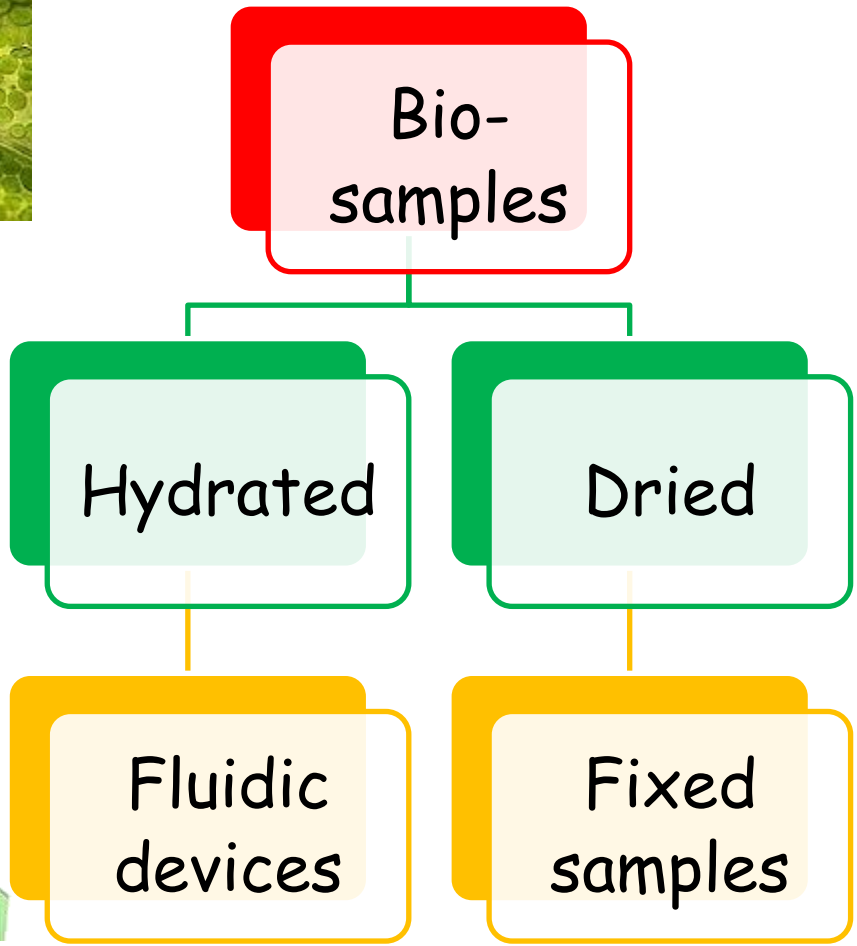

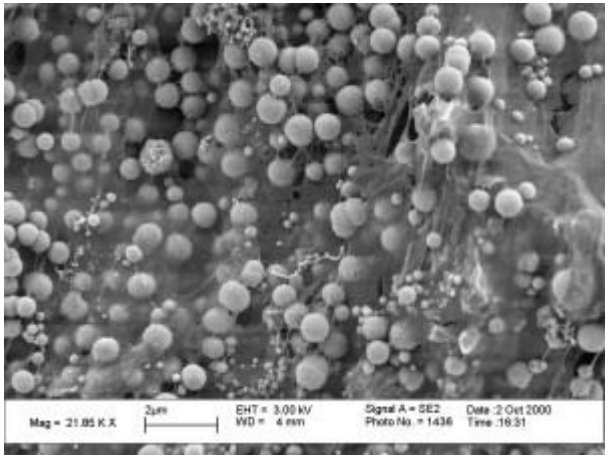

Biofilm, a hydrated matrix of polysaccharide and protein formed by aggregates of bacteria.

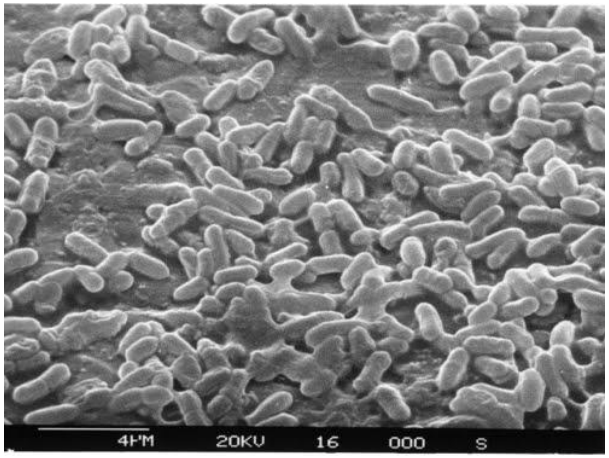

Fixed samples

The aim of fixation is to preserve the structural and biochemical constituents of cells in as close to in vivo conditions as possible

- *Air-drying* can cause collapse of internal cellular structures and activation of cell autolysis (dramatic variation of osmotic pressure within the cells).
- *Flash-freezing* followed by cell lyophilisation (freeze-drying) can not be applied to most common FTIR materials, such as CaF_2 or BaF_2, since too brittle and with poor thermal contact.
- *Alcohol fixation* causes a rapid decrease in cellular volume, caused by the extraction of water from cells. Water is displaced from proteinaceous material, resulting in protein denaturation and organelle disruption. Alcohol extracts lipids from cells but has little effect on carbohydrates.
- *Formalin fixative* has bands potentially overlapping with cellular constituents bands (the most intense peak occurs at 1000 cm^{-1}); however it preserves most lipids and has little impact on carbohydrates. Formalin also appears to preserve protein secondary structure.

Hydrated samples

Hydrated sample measurements have been limited up to now by two major constrains

Manufacture of fluidic devices

The water absorption barrier

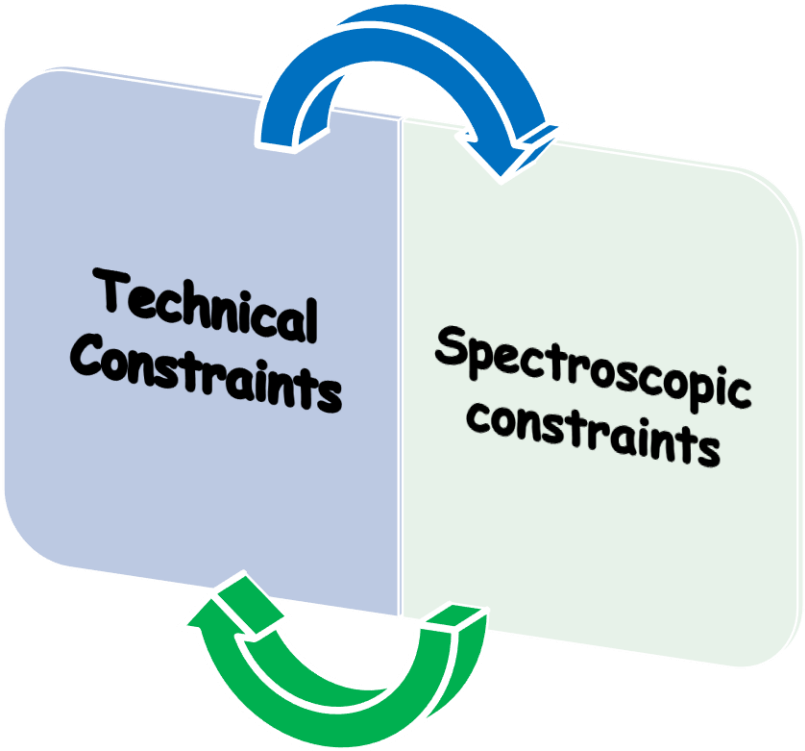

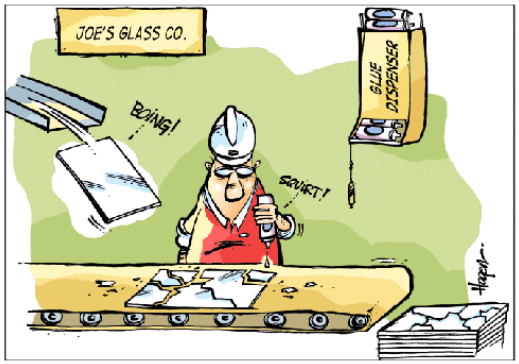

The water absorption barrier

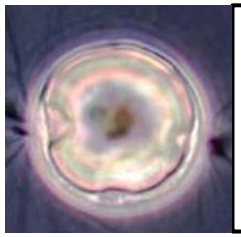

For the sampled volume:
~ 48% extra cellular water
~ 36% intra cellular water
~84% of water

Water: ~ 70% of the cell weight
Dry mass: ~ 50% of proteins
~ 15% of carbohydrates
~ 15% of nucleic acids
~ 10% of lipids
~ 15% other molecules

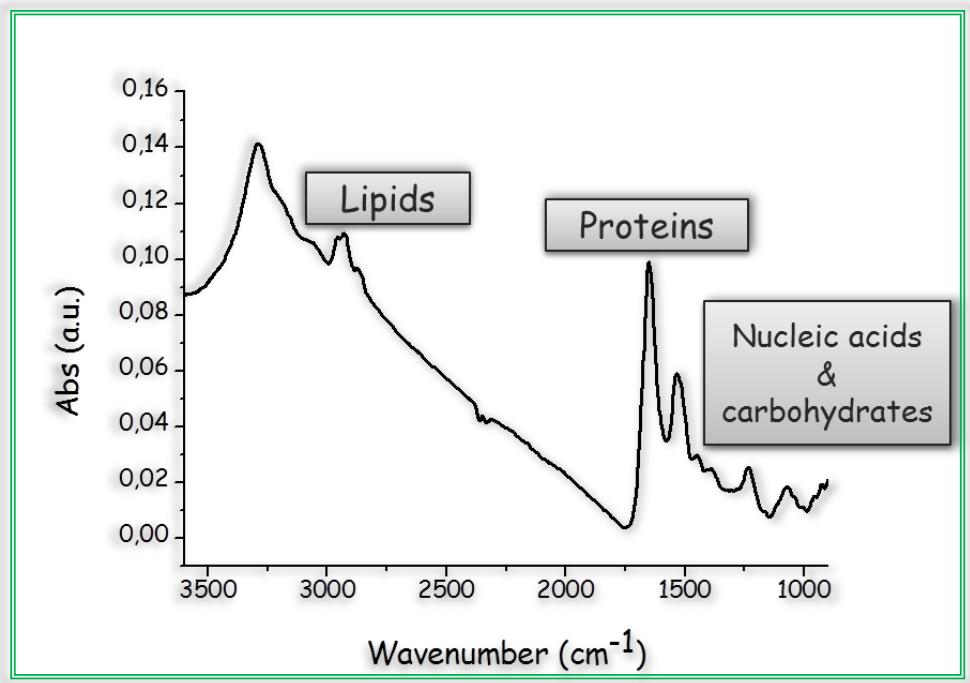

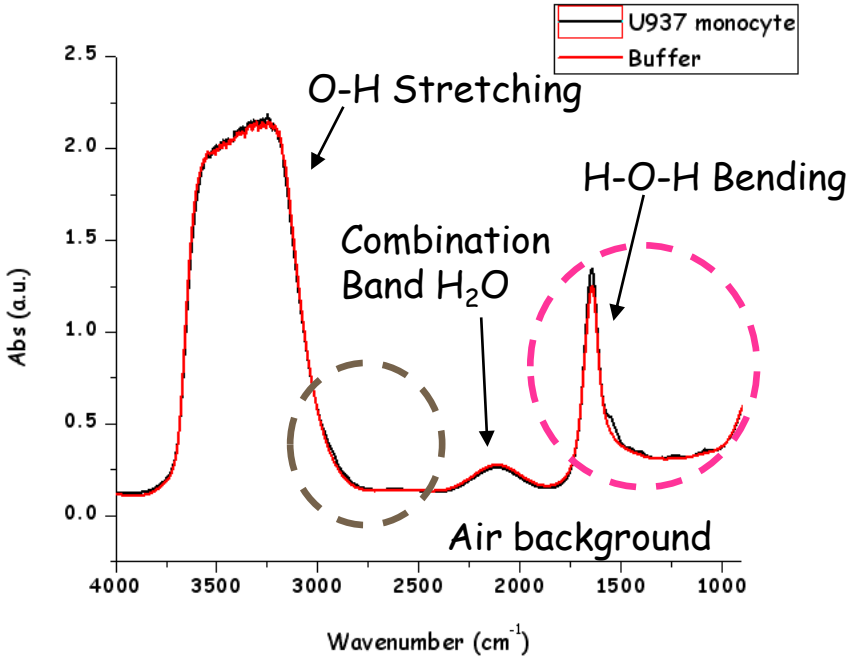

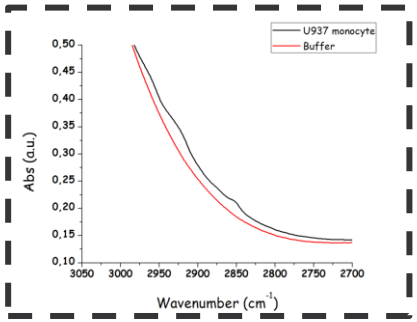

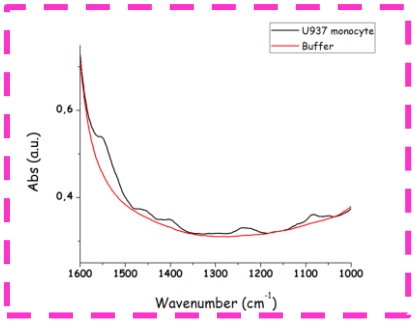

ε_{water} ~ 20 $L \cdot mol^{-1} \cdot cm^{-1}$

$\varepsilon_{Amide\ I} > \varepsilon_{water}$

$[C]_{water} >> [C]_{protein}$

Strategies for living cell sampling

For disclosing cellular IR features, and in particular protein Amide I band, the spectral contribution of water has to be limited:

- By reducing the sampling depth within the cell in ATR mode

  Suitable for prokaryotic cells , very thin adherent cells or special applications where the outermost cell layers are investigated

Micro ATR geometries

From: Sergei G. Kazarian and K. L. Andrew Chan, Analyst, 2013, 138, 1940

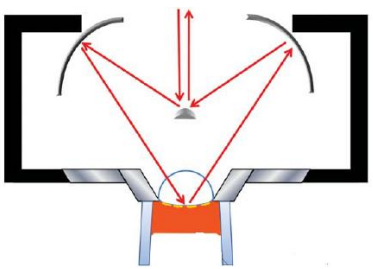

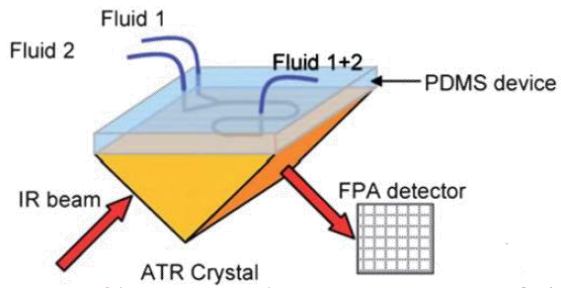

Demountable liquid cell

- By recording transmission (or transflection) spectra of living cells in liquid devices thinner than ~9 microns for avoiding bending water band saturation and allowing water subtraction.
  - Demountable liquid cells, fabricated spacing apart two optical windows, do not assure i-the design flexibility needed for the realization of complex experiments; ii- the accurate control of the optical path, both locally and all over the device
  - A **microfabrication** approach is needed for controlling the water layer thickness and microchannel geometry.

  Materials conventionally employed for IR transmission measurements are not standard for microfabrication

Advantages offered by hydrated unfixed samples

I. Hydrated species, both single cells and tissue section, are closer to the physiological conditions than de-hydrated fixed samples. More relevant biological information can be obtained from their spectra.

Fixatives induce alterations of both content and structure of sample, bio-macromolecules, detectable by IRMS

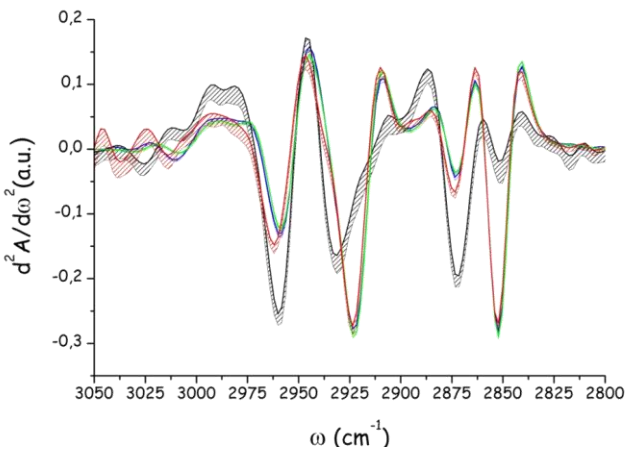

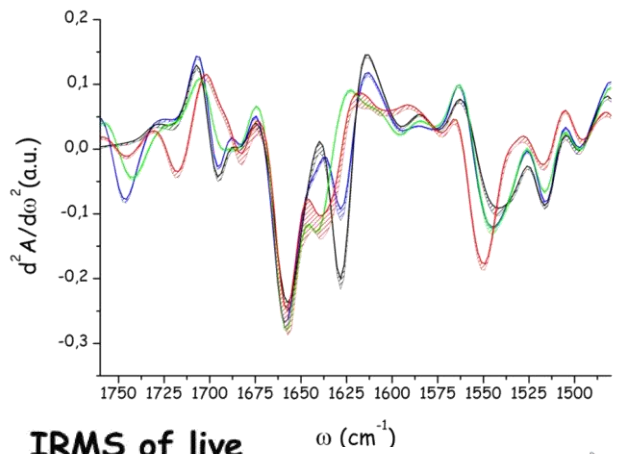

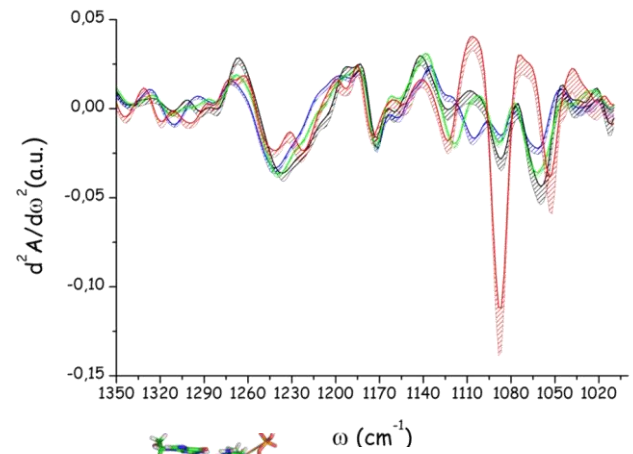

Formalin Air-Dried

Ethanol Living

IRMS of live cells in MD

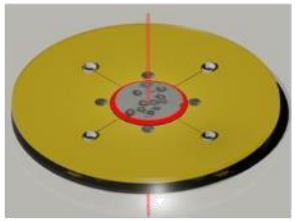

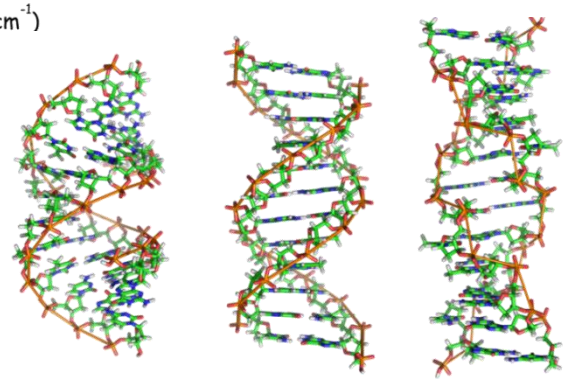

A-DNA B-DNA Z-DNA

L.Vaccari , G. Birarda et al., Anal. Chem. 2012, 84, 4768–4775

Advantages offered by hydrated unfixed samples

II. Dynamic experiments an be performed, in order to monitor the response of a live system under physiological conditions toward different kind of stimuli

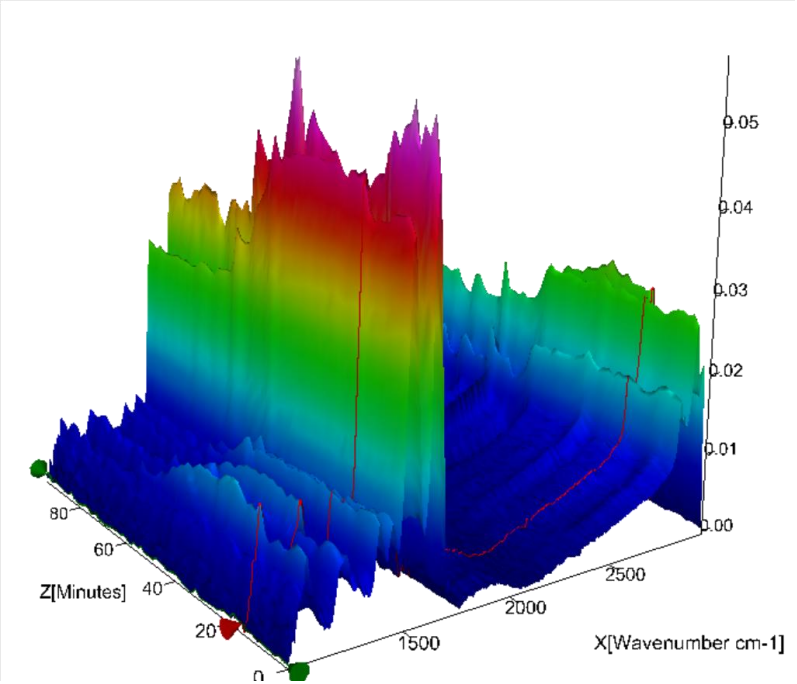

III. For transmission (or transflection) experiments, the closer matching between the refractive index of cell and water produces a great suppression of the scattering effects that dramatically affect single fixed cell spectra

Data acquisition

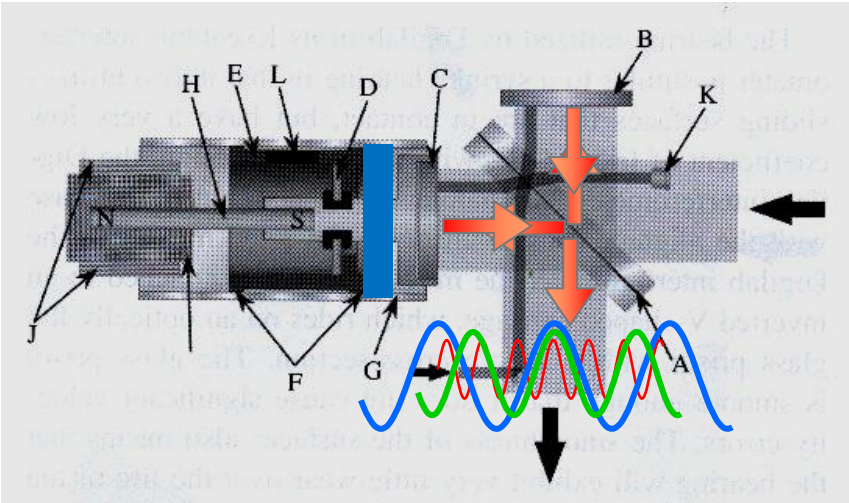

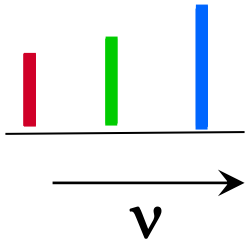

Sample Single channel

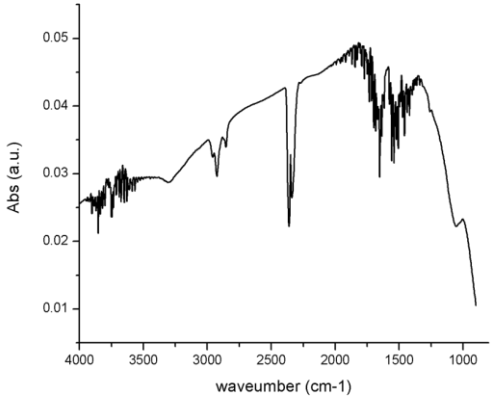

Reference Single channel

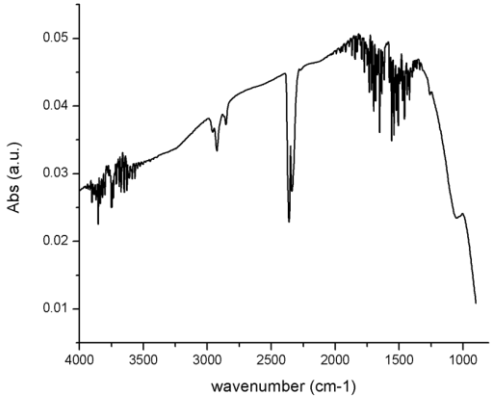

Fast Fourier Transform

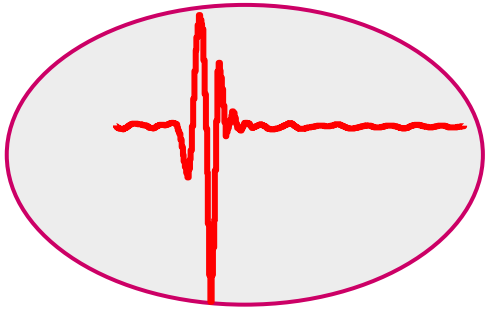

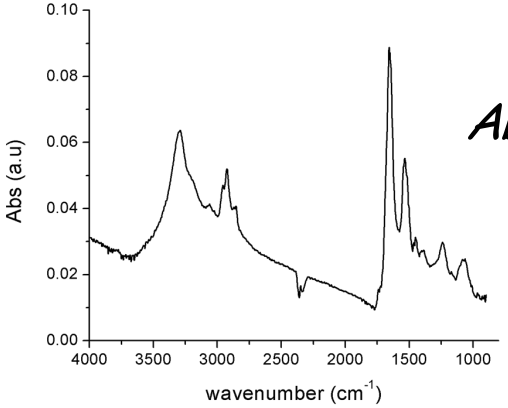

$$Abs = -\log\left(\frac{SSC}{RSC}\right)$$

Data preprocessing- Atmospheric compensation

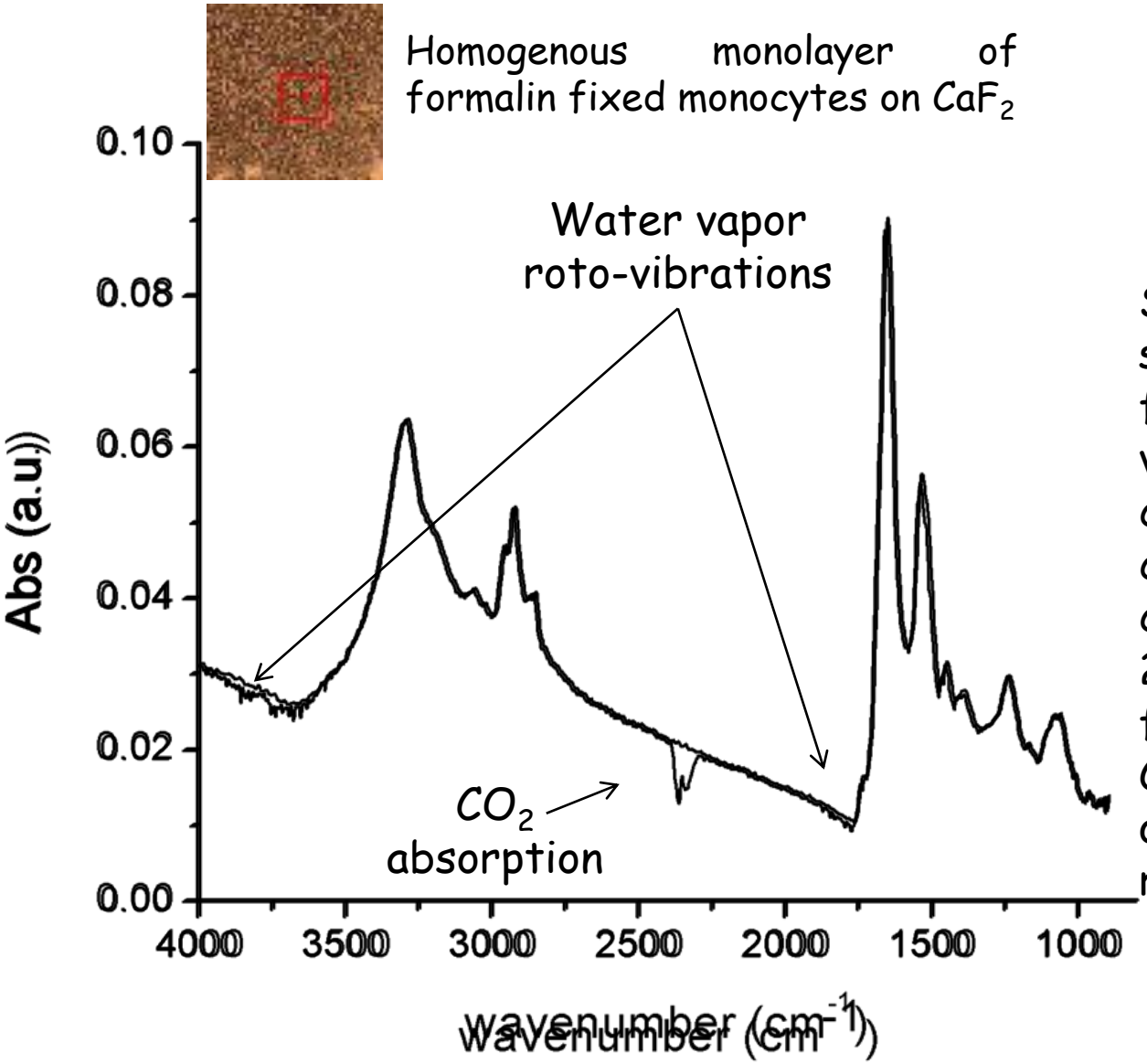

Atmospheric compensated Spectrum

Spectral regions free of sample bands are used for evaluating water vapor and carbon dioxide content: 3600 to 4000 cm^{-1} region for H_2O compensation, and 2300 to 2400 cm^{-1} region for CO_2.
Correction is extended over the entire spectral range.

Data preprocessing- Spectral smoothing

Noise reduction: spectral smoothing
Savitzky-Golay method, K+1 smoothing points

The method essentially performs a local polynomial regression (of degree k) on a series of values (k+1 points, equally spaced in the series) to determine the smoothed value for each point.

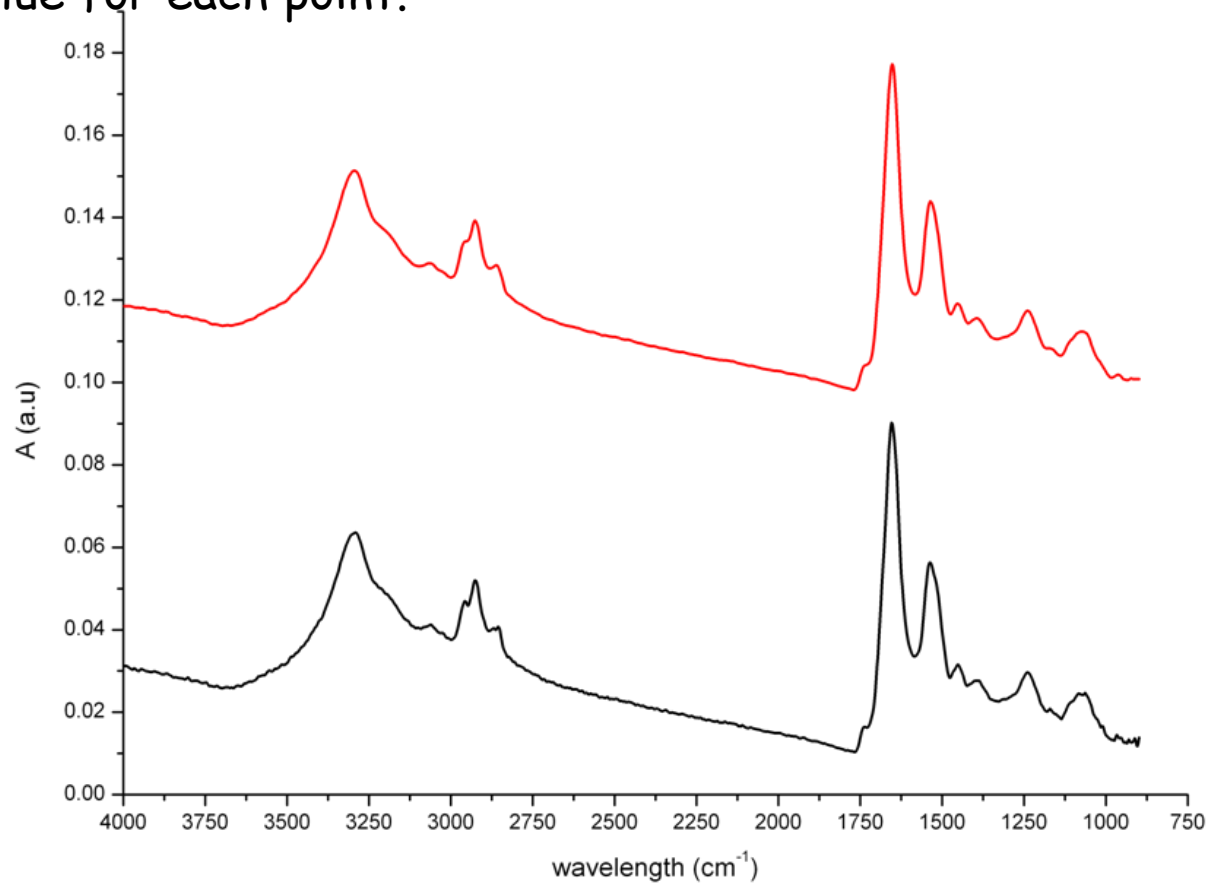

Data preprocessing- Good Laboratory Practice

However, algorithms are NEVER better than GOOD LABORATORY PRACTICE!

Water vapor and carbon dioxide spectral contributions as well as the spectral noise should be reduced:

- Purging the interferometer with N_2/dry air or operating in vacuum
- Purging the microscope stage with N_2/ dry air
- With a good conditioning of the laboratory environment

Too many people around the microscope!

- Implementing the S/N spectral ratio
    - Increasing the number of scans
    - Increasing the signal -> Brighter Sources -> Synchrotron Radiation
    - Reducing any possible source of noise: vibrations, electronic noise, …..

Data preprocessing- Mie Scattering correction

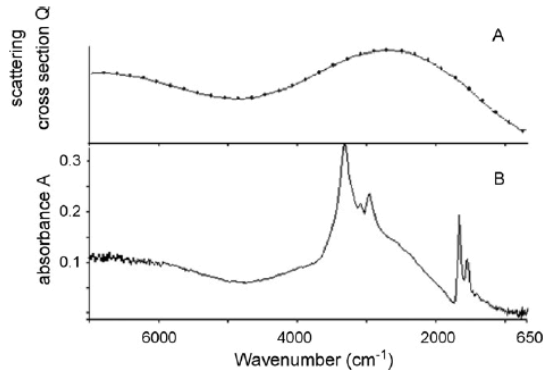

B. Mohlenhoff et al, Biophysical Journal, 2005, 88, 3635-3640

Single cell spectra often present slow oscillations of the baseline. The origin is related to Mie-type scattering, which takes place when the wavelength of the incident radiation is similar to the one of the scattering particles.

→ **Position and intensity of IR bands can be affected**

EMSC (Extended multiplicative scattering correction) corrects for these effects modeling the scattering object as a non-absorbing dielectric sphere..

$$Q = 2 - \left(\frac{4}{\rho}\right)\sin\rho + \left(\frac{4}{\rho^2}\right)[1 - \cos\rho]$$

$$\rho = 4\pi d(n-1)/\lambda$$

Q Scattering efficiency
d diameter of the sphere
$n=n_1/n_2$= refractive index of sphere and surrounding medium

Resonant Mie scattering: scattering with simultaneous absorption

Paul Bassan,, Hugh J. Byrne at al., Analyst, 2009, 134(6), 1171-1175
Paul Bassan, Achim Kohler, Analyst, 2010, 135, 68-277

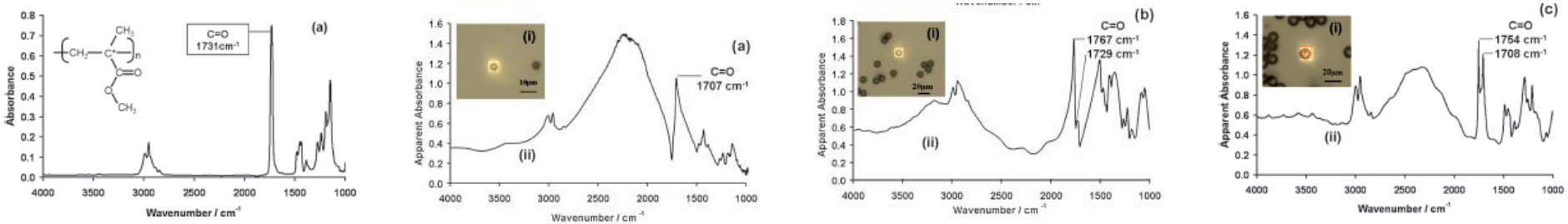

Spectra of isolated single cells often exhibit significant **distortions of the band shapes**, especially a sort of derivative-like distortion on the high wavenumber side of the Amide I band.
RMieS correction have been developed but still to be fully optimized.

Data pre-processing- Spectra derivative

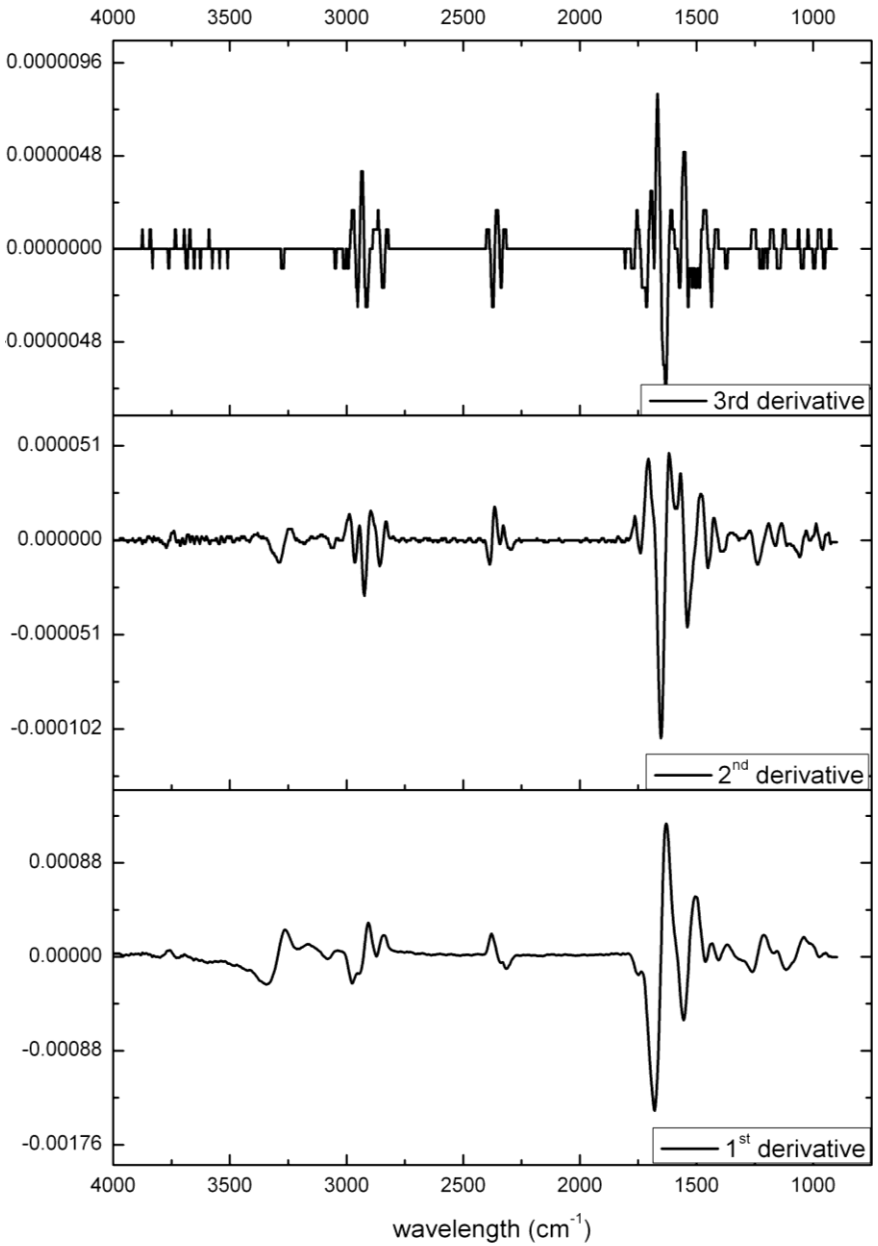

By using the derivative spectra, it is possible to minimize baseline variations and maximize spectral resolution. The derivative brings the overlapping peaks apart and the linear background becomes to a constant level.

In parallel, the spectral noise is also magnified, and the spectral complexity as well. Therefore, usually derivative algorithms take place with smoothing, commonly Savitzky-Golay.

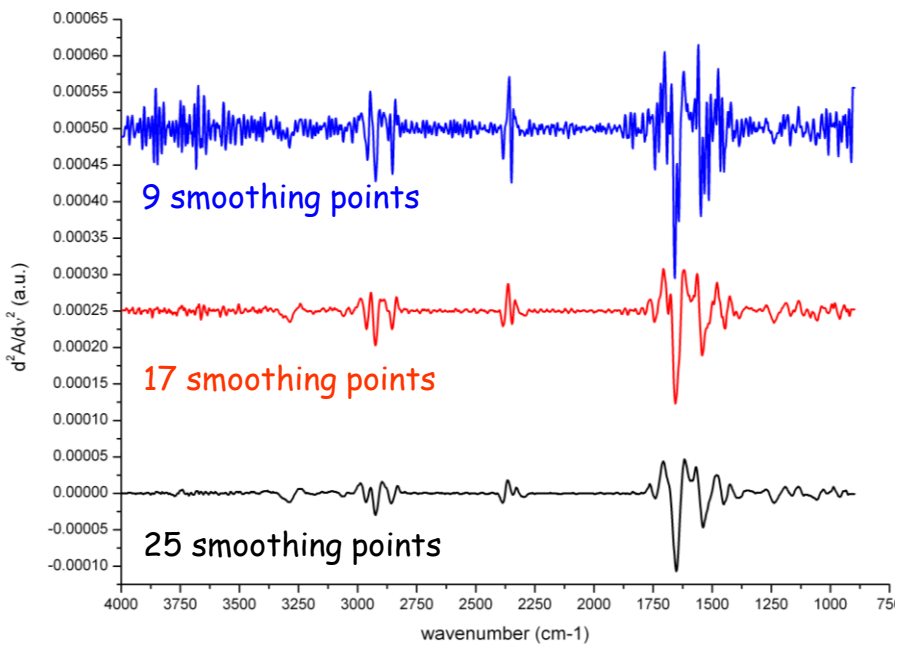

Data pre-processing- Spectra Normalization

The goal of normalization is to perform numerically what was not able to be performed physically during data collection; that is, recover exact replicates when no bio-logical differences exist. Normalization methods preserve the spectral shape, making easier the data analysis, but results depend on the spectral range.

Constant shift – offset correction

When the replicates exhibit a simple vertical offset between spectra, normalization is achieved by subtracting a sample-specific constant from each.

Scaling – Vector Normalization

If each spectrum of a data set contains a different amount of energy, large intensities are magnified more than low intensities. The scaling procedure produces a set of unit-length vectors in the wavelength space. For example, normalization allows to remove spectral intensity variations due to variation in sample thickness.

$$A_i(vector\ normalizaed) = \frac{A_i}{\|Ai\|}$$

Standard Normal Variate (SNV)

SNV allows both spectral centering, since it produces mean-zero spectra, and their scaling

$$A_{ik}(SVN) = \frac{A_{ik} - \overline{A_i}}{\sqrt{\frac{\sum_{k=1}^{p}(A_{ik} - \overline{A_i})^2}{p-1}}}$$

A_{ik}=SNV absorbance of the i-spectrum at λ_k
p= number of spectral points
A_i = Average absorbance for all the λ_k (spectrum mean)

Data Analysis

Spectra comparison

Spectral analysis "by visual inspection"

For small data sets (few spectra), spectra can be compared "visually" in order to highlight spectral similarities and/or differences affecting:

- Band position (band shifts), width (band broadening), shape (band components) and intensity.
- Ratios of peak areas (different proportion of most fundamental tissue-cell constituents).

The reliability of biological conclusions drawn out from an experiment relies on the measurements of a statistically relevant number of samples.

Statistical analysis

Univariate and multivariate statistical analysis methods allow to compare a huge amount of spectra simultaneously, classifying them on the base of spectral similarities, affinities.

Univariate Methods: Average, standard deviation, regression techniques (PLS,....)

Multivariate Methods: **Cluster Analysis**, **Principal Component analysis** (**PCA**), ...

1- Cluster Analysis

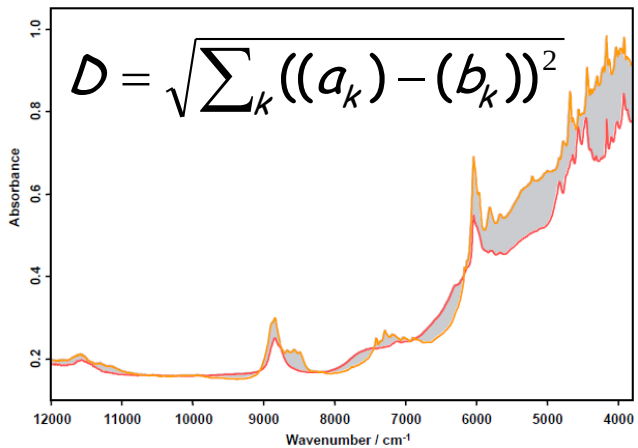

1. Spectral distance calculation

Distance between spectra *a* and *b* can be calculated with many algorithms.

Euclidean spectral distance between *a* and *b* spectra is calculated over the all sampled *k* points.

2. Spectral distance matrix

	a	b	c	d	e
a	0				
b	44	0			
c	11	54	0		
d	100	68	97	0	
e	120	92	115	21	0

There are many methods available to calculate spectral distances between a newly-created cluster and all the other spectra or clusters.

N	Clusters
1	a-b-c-d-e
2	ac-b-d-e
3	ac-b-de
4	abc-de
5	abcde

3. Spectra clustering

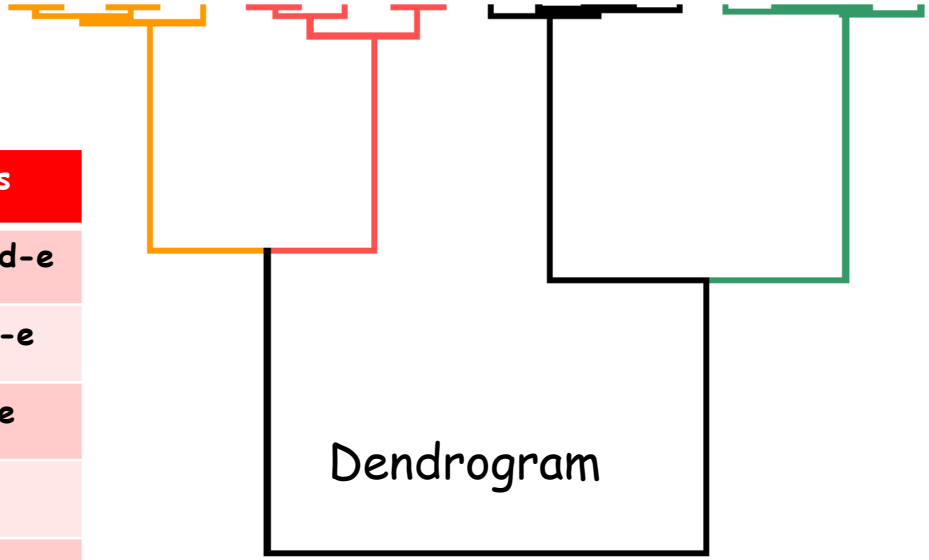

2- PCA – Principal component Analysis

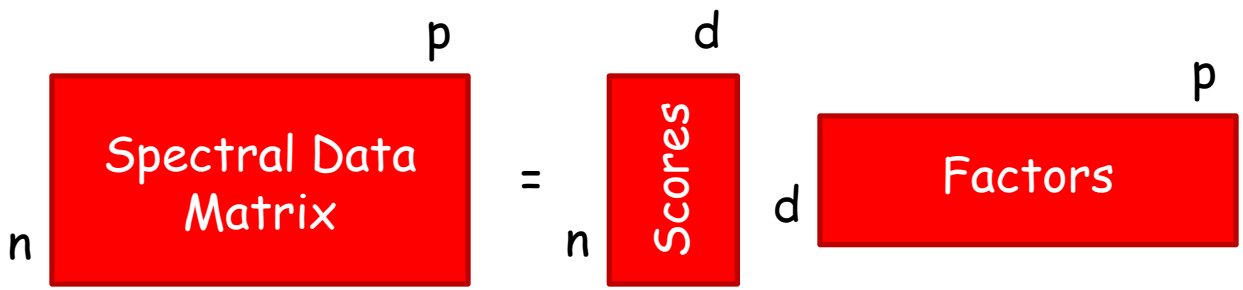

n spectra with p data points; d scores for each spectrum (d<n); d factors with p data points (d<n)

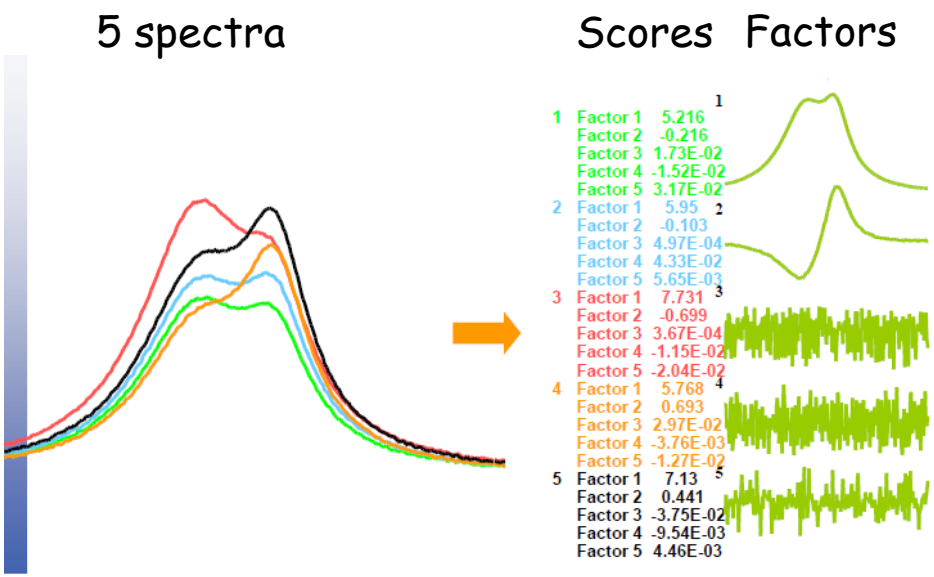

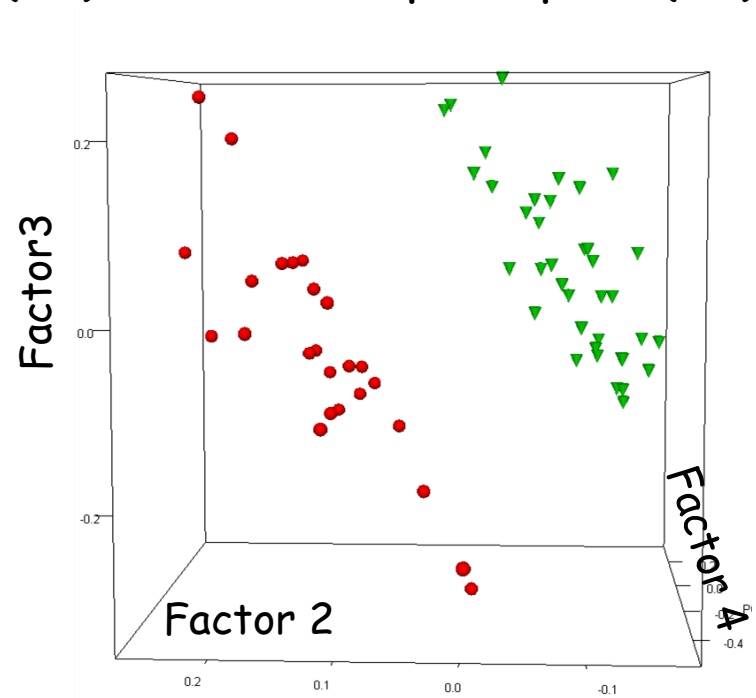

In Situ FT-IR Microscopic Study on Enzymatic Treatment of poplar Wood Cross-Sections

N. Gierlinger et al., Biomacromolecules 2008, 9, 2194-2201

Cellulose is the major polymeric component of the plant matter and is the most abundant polysaccharide in Earth.

Biofuels from Cellulosic Biomass

Purpose is to convert cellulosic biomass to fuels such as ethanol, methanol, dimethyl ether, or gasoline.

Poplar are a common source of clean biomass

Enzymatic conversion → Glucose

Cellulases

↓ Fermentation

Ethanol

The rate of efficiency of cellulose hydrolysis is affected by many factors: enzymatic system, substrate characteristics (degree of polymerization, crystallinity, pore size) and cellulose association with hemicellulose and lignin.

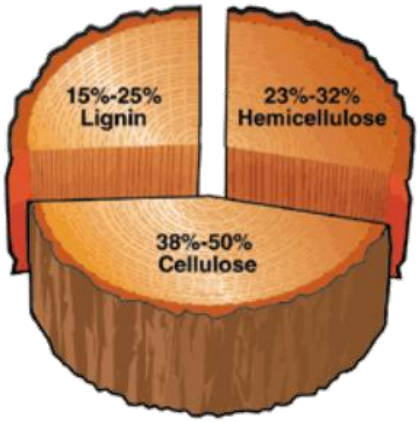

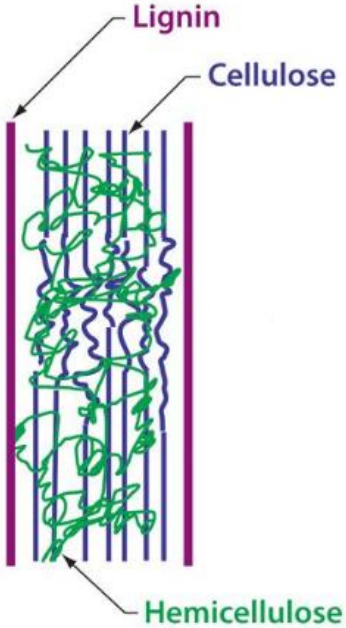

Within a plant cell wall, cellulose is embedded in a matrix of other polysaccharides (hemicellulose) and lignin

Cellulose

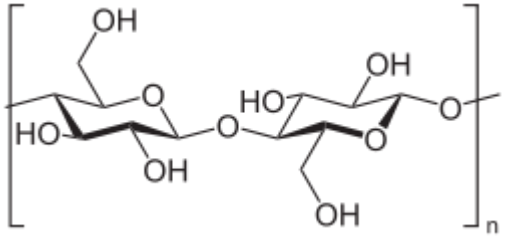

Cellulose is a homopolymer of glucose consisting of β(1-4) bonds. It differs from another polymer of glucose, starch that consists of α(1-4) bonds

Lignin is a complex chemical compound most commonly derived from wood. It is a racemic, heteropolymer consisting of three hydroxycinnamyl alcohol monomers differing in their degree of methoxylation

Hemicellulose: Heteropolymer of pentoses (xylose and arabinose) and hexoses (glucose, galactose, mannose) and sugar acids (acetic).

Hemicellulose

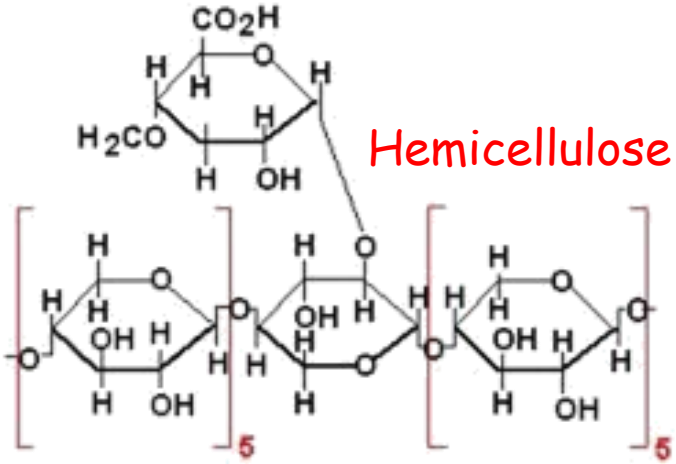

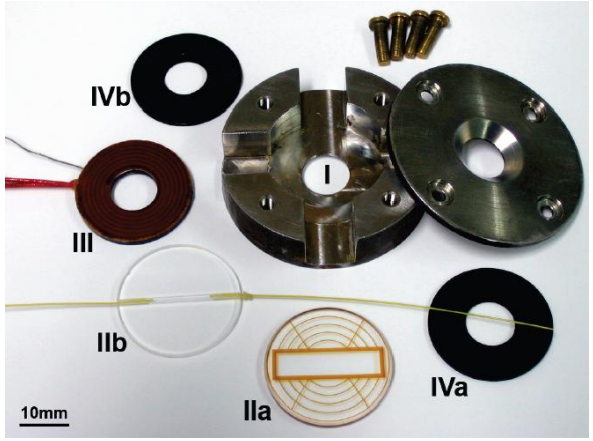

The enzymatic degradation of polar wood samples induced by a multicomponent commercial enzyme has been studied. A fluidic cell with 10 micron optical path has been used that allows i- T control and ii- waste removal. Both normal (N) and tension (T) wood have been considered.

Tension wood is a type of wood which forms in angiosperms in response to environmental stresses. It is characterized by a gelatinous cellulose layer, G-layer, and has an extra 50% cellulose content with respect to normal wood. For the tree, the purpose of tension wood is to help the tree stay stable, and to keep the tree upright. This type of wood is not useful for people who work with wood to make flooring, furniture, and other products, because it has an irregular texture, but it should be ideal for biomass synthesis.

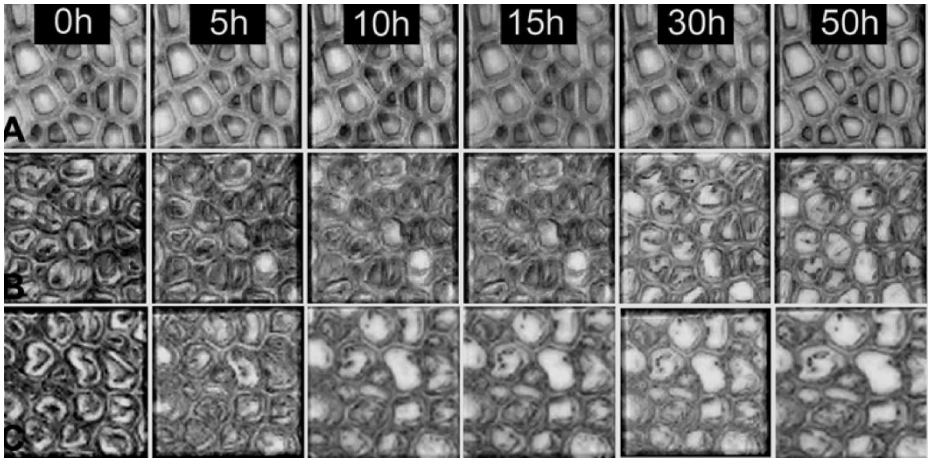

NW, 22°C

TW, 22°C

TW, 50°C

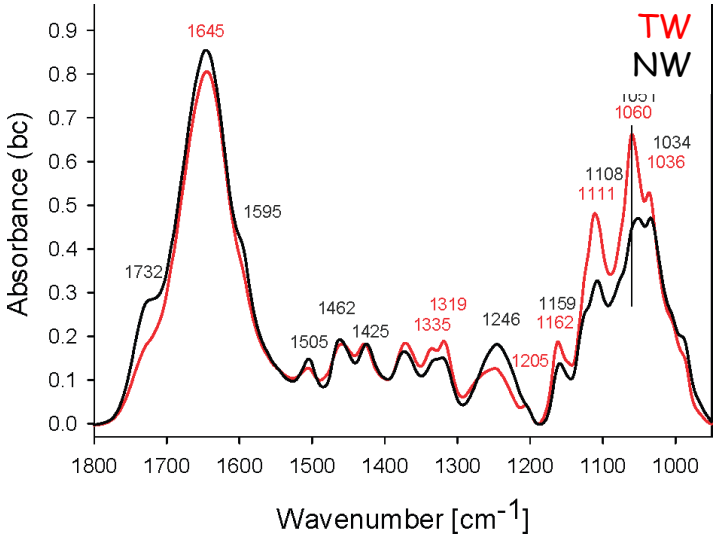

TW and NW have peculiar spectral patterns

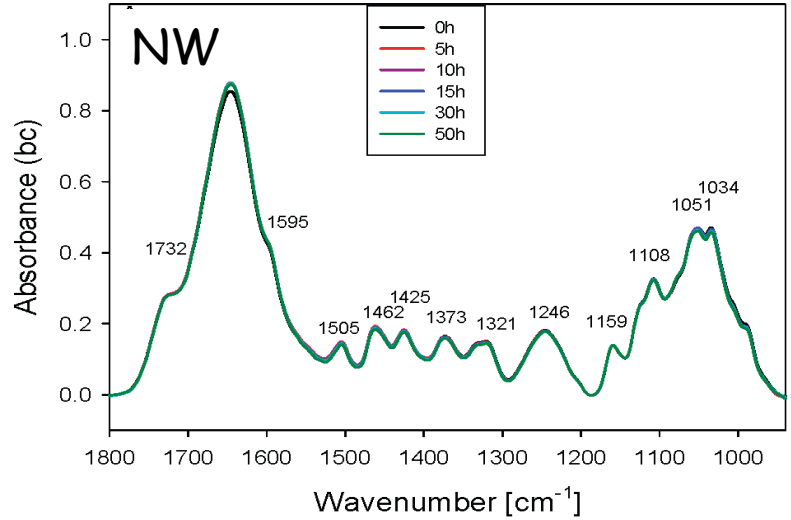

NW spectra does not change in time. The enzyme is barely efficient toward cellulose of cell walls

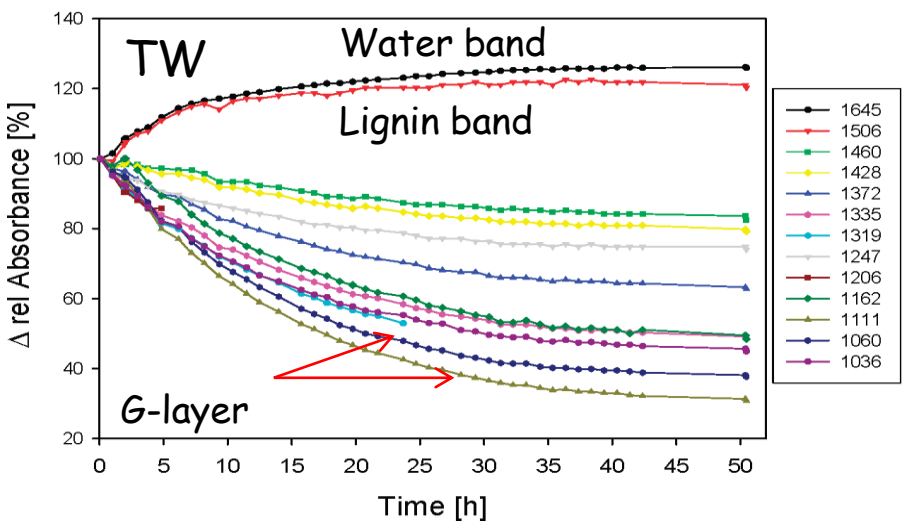

TW bands mostly affected by cellulase enzymes are related to G-layers

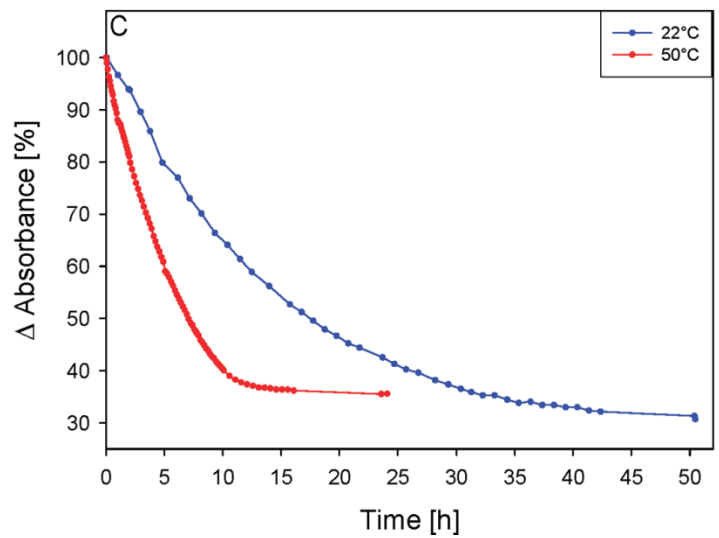

Temperature is reducing to almost 1/3 the degradation time of G-layer in TW

Real-time Chemical imaging of bacterial activity in biofilms

From H-Y H. Holman et al., Analytical Chemistry, 81:8564 (2009)

"Bacterial biofilms are structured dynamic communities of aggregated cells enclosed in a self-produced polymeric matrix that adheres to both inert and living surfaces in aqueous environments."

http://www.lcs.syr.edu/academic/biochem_engineering/research_areas/biomaterials_tissue_engineering.aspx

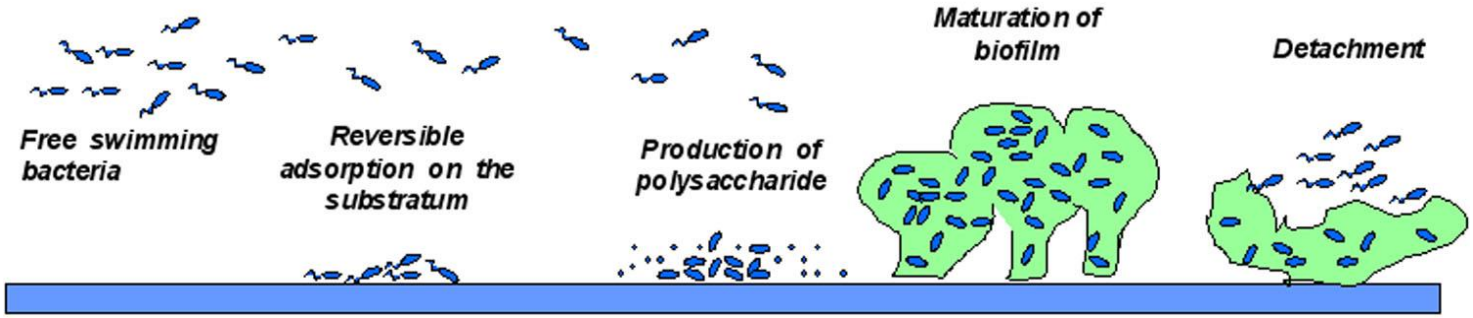

"When opportunistic pathogenic bacteria develop biofilms, they can become up to 1000 times more resistant to antibiotics. The formation of biofilms and their resistance to antibiotics and host immune attacks are at the root of many persistent and chronic bacterial infections. Real time monitoring of bacterial activity at a chemical level during biofilm initiation, growth, release and bacteria-drug interactions in real time as the processes are happening could lead to new preventive and curative treatments."

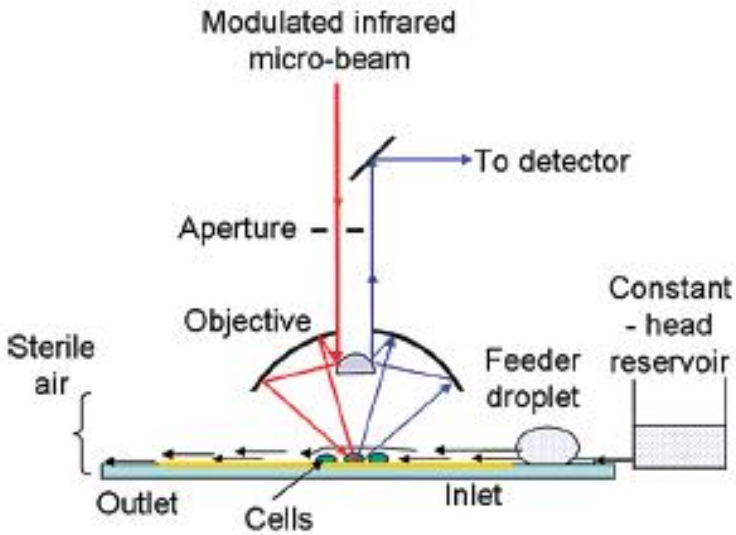

Uptake of mitomycin-C (MMC) by Escherichia coli within a biofilm

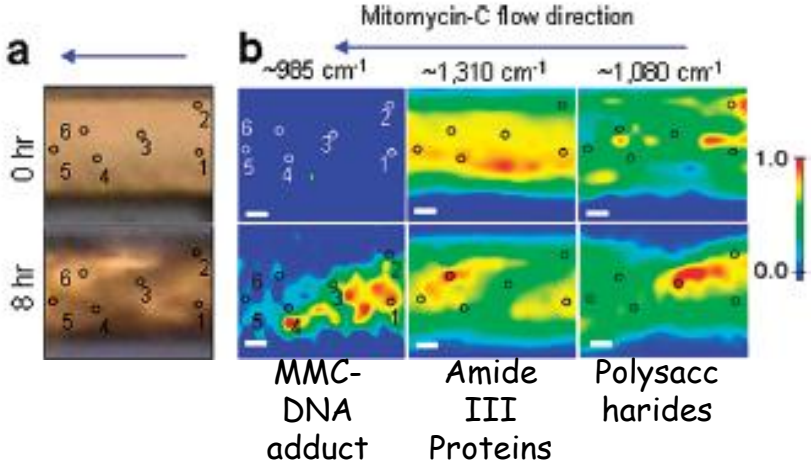

In points 1 and 2 (closer to MMC source) as well as 3 and 4 (Amide III richer) → Higher concentrations of MMC-DNA adduct
In points 2 and 3, increased polysaccharides and decreased Amide III
In point 6 (lower concentration of MMC-DNA adduct) the Amide II signal increases.

Cellular diversification processes in response to MMC toxicity

Dynamics of biofilm formation in micro-channels

1080 cm^{-1} polysaccharide
1130 cm^{-1} glycocalyx
Glycocalyx refers to extracellular glycoprotein produced by some bacteria
1240 cm^{-1} DNA/RNA
1310 cm^{-1} Amide III

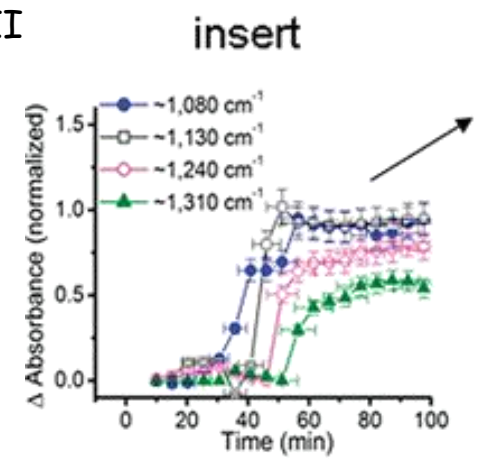

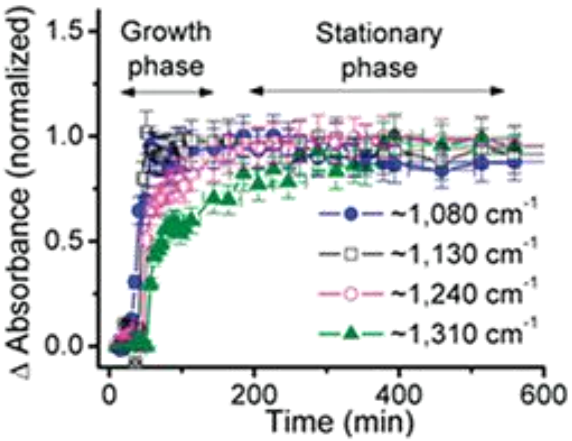

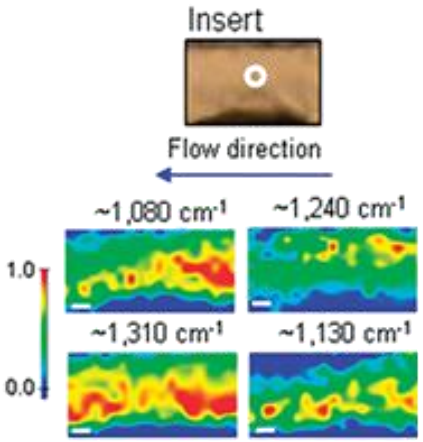

Strong correlation among different carbohydrates, glycocalyx and Amide III bands. Glycocalyx synthesis is prerequisite for the formation of stable bacterial biofilms

Prion disorders

Aberrant metabolism of the Prion Protein (PrP)

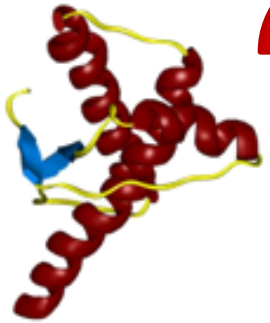

PrP^{C}
Alpha-helical
Protease sensitive

PrP^{SC} - PrP^{CJD}
beta- plated sheet
Protease resistant

Prion rods

PNAS 1999 vol. 96 no. 26 15137-15142

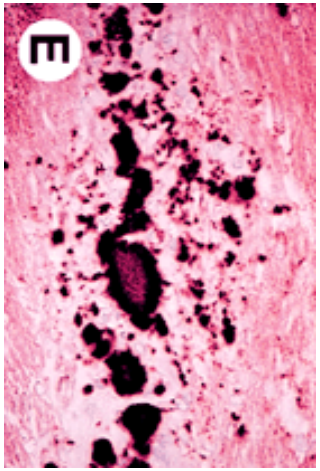

PNAS 1998 vol. 95 no. 23 13363-13383

PrP amyloid plaques

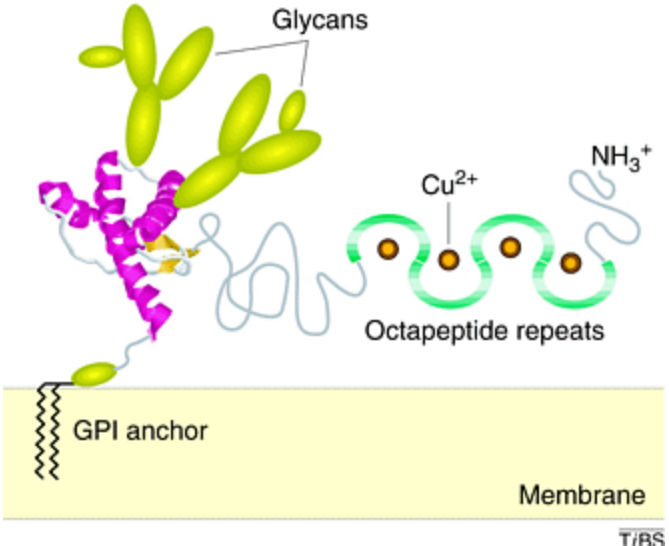

SR-IRMS and prion research

- ✓ FTIR spectroscopy has been largely employed for studying the conformational changes associated to the conversion of PrP^{C} into PrP^{Sc}

PrP^{C} 42% α-helix; 3% β-sheet // PrP^{Sc} < α-helix; > β-sheet Phenotype dependent

- ✓ IRMS is able to distinguish between scrapie (S) and normal (N) brain tissues but the spectroscopic differences between different cerebellar substructures are much pronounced than disease alterations.

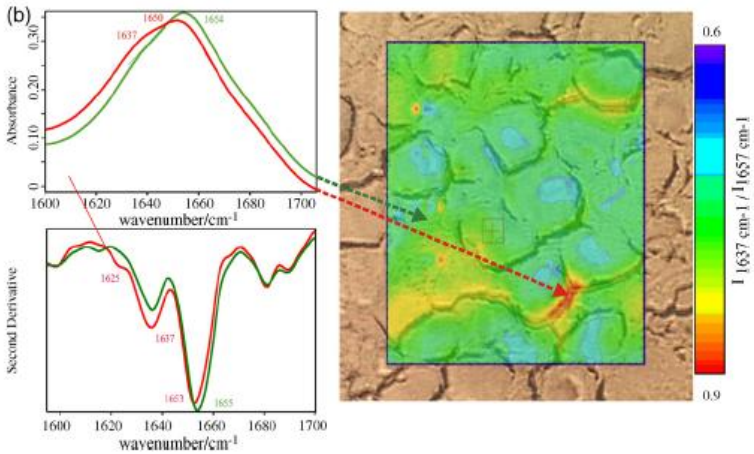

Differentiation is based on the superimposition of multiple contribution more than on the identification of structural protein alteration, evidenced only but not always in terminally ill animals (Dilution effect)

Tissue architecture complexity is limiting the understanding of cellular bases of disease

A. Kretlow wt al., FTIR-microspectroscopy of prion-infected nervous tissue, *Biochimica et Biophysica Acata (BBA) – Biomembranes* (2006), 7:948-959

M. Beekes et al., Analytical applications of Fourirer transform-infrared (FT-IR) spectroscopy in microbiology and Prion research, *Veterinary microbiology* (2007), 123:305-319

SR-IRMS and prion research: a cellular study

IRMS is a sensitive single-cell diagnostic tool for testing prion infection, faster than conventional Western blot PK digestion assay

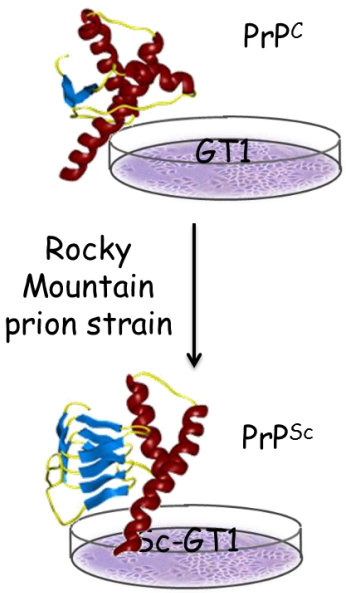

▪Multiple cell sensitivity
▪Execution time: many hours

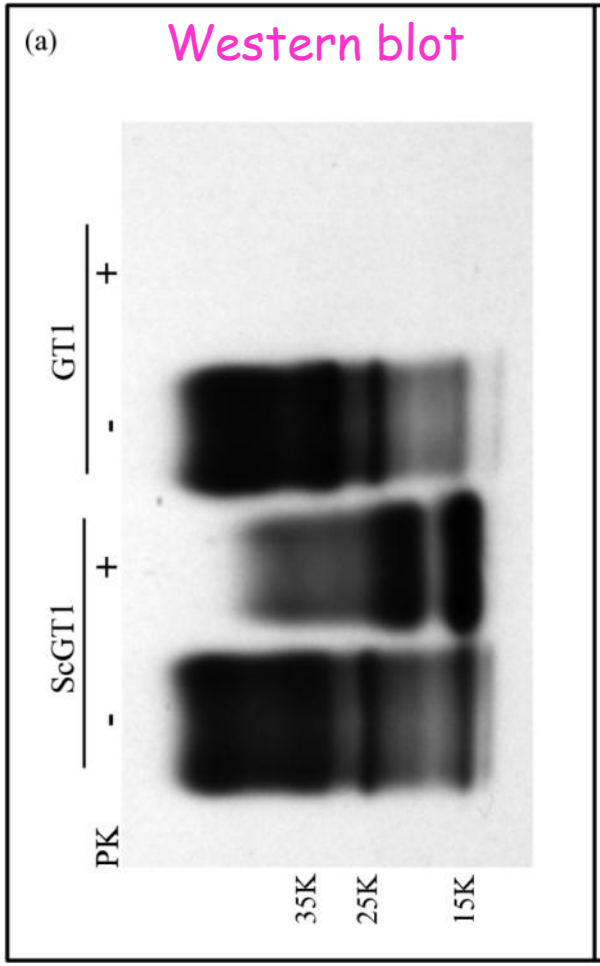

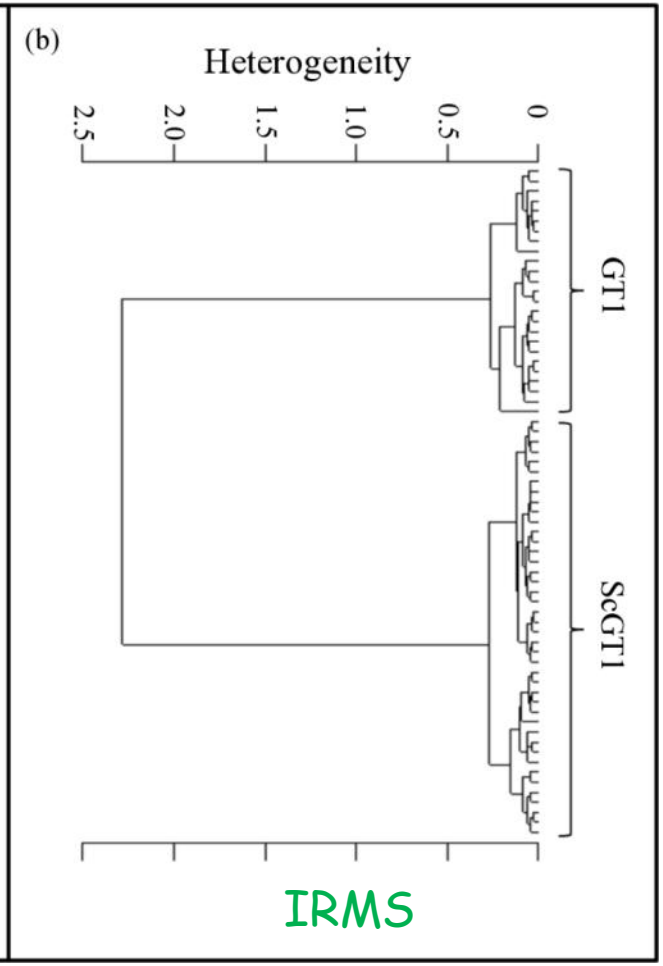

▪Single cell sensitivity
▪Execution time: few minutes

A. Didonna, L. Vaccari, et al., *ACS Chemical Neuroscience* 2011 2 (3), 160-174

IRMS revealed the biochemical reasons of classification

- Increase Glu and Asp protonated aminoacid

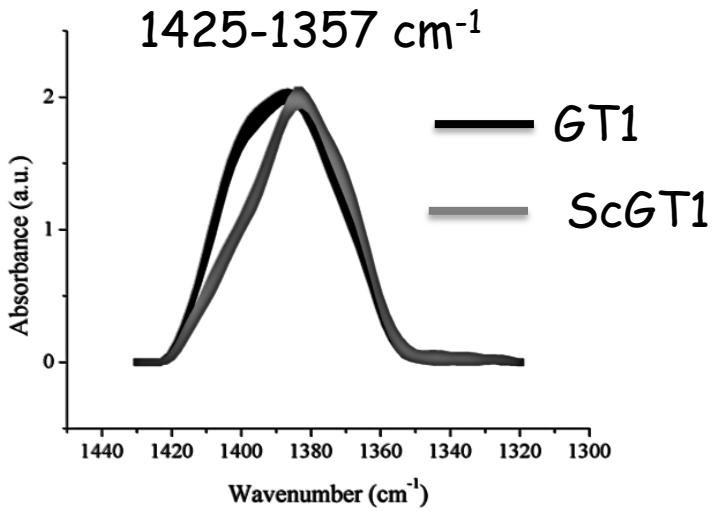

- Down-regulation in protein and lipid synthesis upon prion infection was elicited by semi-quantitative analysis

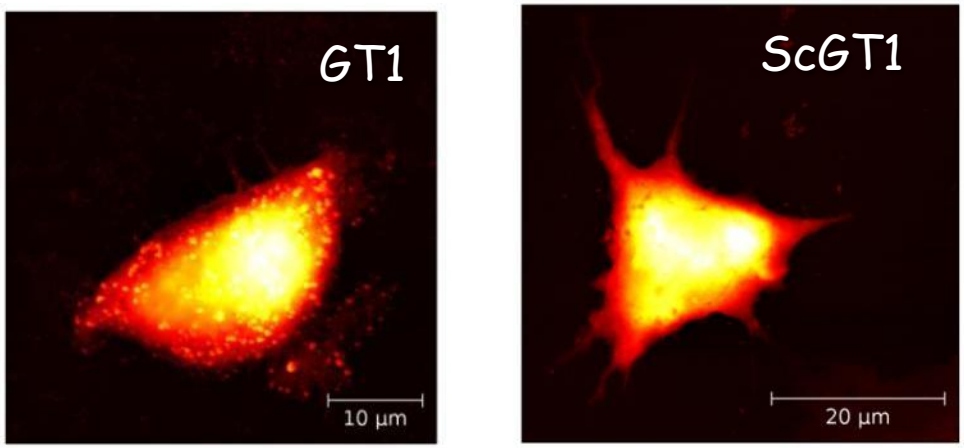

AFM: GT1 and Sc-GT1 have comparable pyramid like shape and effective cell height

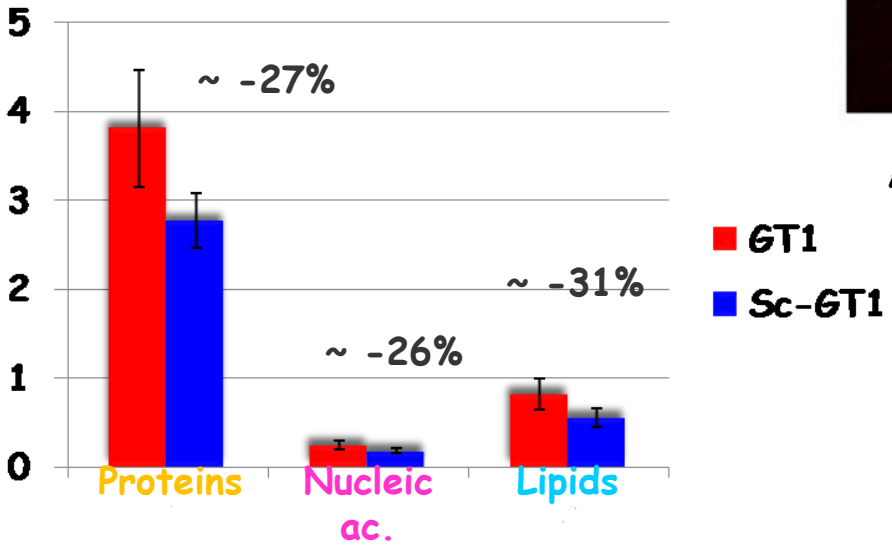

IRMS revealed an increase in both number and dimension of lysosomal compartments upon prion infection

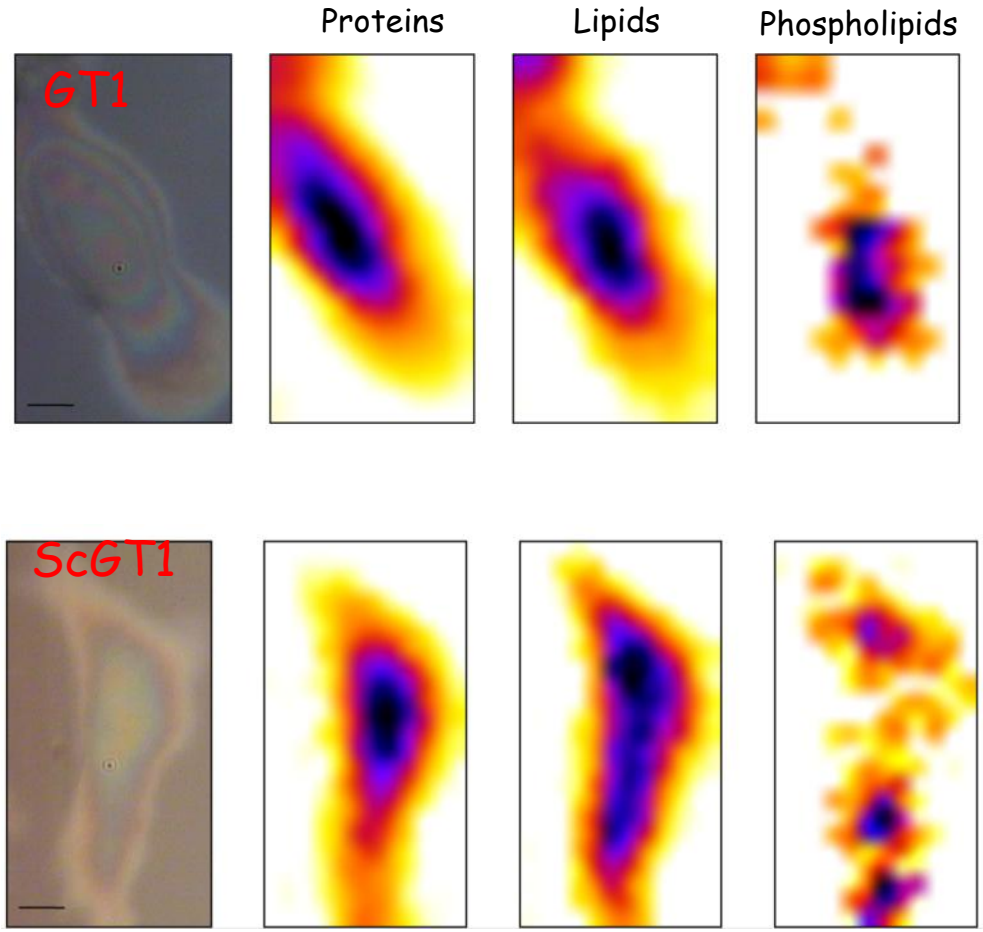

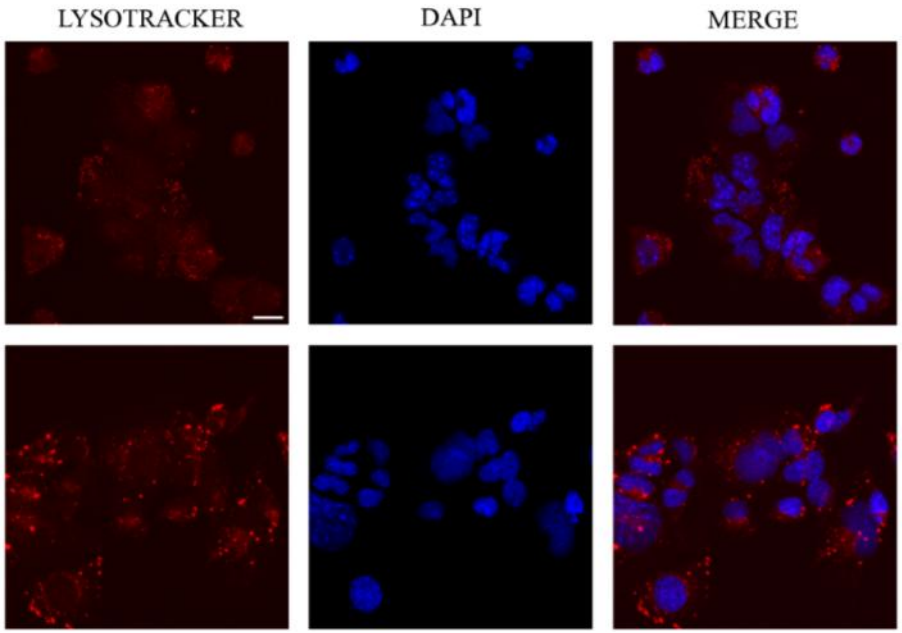

The synergic matching of IRMS with complementary investigation tools is a winning strategy for shining a light on cellular phenomena behind prion infection

YOUR EXPERIMENT

The sample

Root thin sample slides deposited on TEM grids

Data Acquisition

FTIR imaging with conventional source and FPA detector

IRSR with single point MCT detector (Mapping of small areas)

Data pre-treatment

Data Analysis

Univariate data analysis (band integration)

HCA

PCA

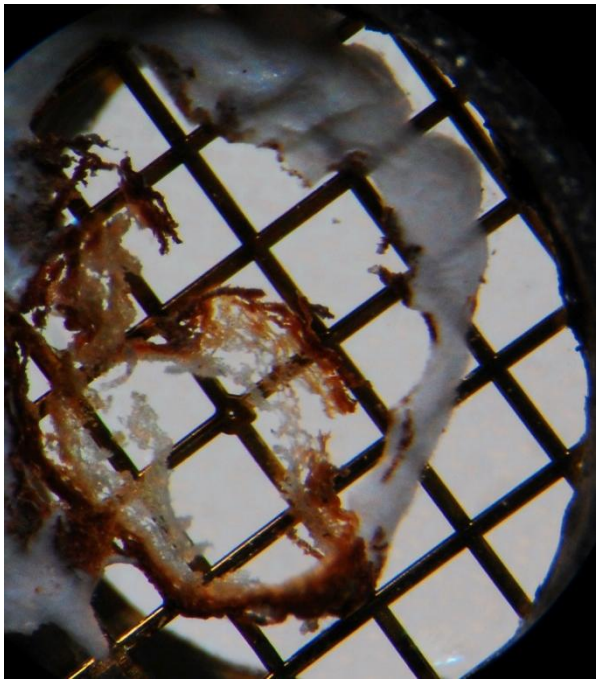

Sample regions exposed and non to X-rays will be monitored. The radiation damage effects will be considered